Journal of Comparative Neurology

WILEY

JCN RESEARCH IN SYSTEMS NEUROSCIENCE THE JOURNAL OF COMPARATIVE NEUROLOGY

RESEARCH ARTICLE OPEN ACCESS

Stereological Analysis of the Rhesus Monkey Perirhinal and Parahippocampal Cortices

Justine Villard[1] | Loïc J. Chareyron[1,2] | Pamela Banta Lavenex[1,3] | David G. Amaral[4,5] | Pierre Lavenex[1]

[1]Laboratory of Brain and Cognitive Development, Institute of Psychology, University of Lausanne, Lausanne, Switzerland | [2]Cognitive Neuroscience and Neuropsychiatry, Developmental Neurosciences, University College London Great Ormond Street Institute of Child Health, London, UK | [3]Faculty of Psychology, UniDistance Suisse, Brig, Switzerland | [4]MIND Institute and Department of Psychiatry and Behavioral Sciences, University of California at Davis, Davis, California, USA | [5]California National Primate Research Center, University of California at Davis, Davis, California, USA

Correspondence: Pierre Lavenex (pierre.lavenex@unil.ch)

Received: 10 June 2024 | **Revised:** 3 October 2024 | **Accepted:** 23 October 2024

Funding: This work was supported by the Swiss National Science Foundation (Grants P00A-106701, PP00P3-124536, and 310030_143956), the US National Institutes of Health (Grants MH041479 and NS16980), and the California National Primate Research Center (Grant OD011107).

Keywords: brain organization | consolidation | hierarchy | hippocampal formation | medial temporal lobe | memory | neuron number | perception

ABSTRACT

The perirhinal and parahippocampal cortices are key components of the medial temporal lobe memory system. Despite their essential roles in mnemonic and perceptual functions, there is limited quantitative information regarding their structural characteristics. Here, we implemented design-based stereological techniques to provide estimates of neuron number, neuronal soma size, and volume of the different layers and subdivisions of the perirhinal and parahippocampal cortices in adult macaque monkeys (*Macaca mulatta*, 5–9 years of age). We found that areas 36r and 36c of the perirhinal cortex and areas TF and TH of the parahippocampal cortex exhibit relatively large superficial layers, which are characteristic of the laminar organization of higher order associational cortices. In contrast, area 35 of the perirhinal cortex exhibits relatively large deep layers. Although neuronal soma size varies between subdivisions and layers, neurons are generally larger in the perirhinal cortex than in the parahippocampal cortex and even larger in the entorhinal cortex. These morphological characteristics are consistent with the hierarchical organization of these cortices within the medial temporal lobe. Comparing data in rats, monkeys, and humans, we found species differences in the relative size of these structures, showing that the perirhinal and parahippocampal cortices have expanded in parallel to the cerebral cortex and may play a greater role in the integration of information in the neocortical–hippocampal loop in primates. Altogether, these normative data provide an essential reference to extrapolate findings from experimental studies in animals and create realistic models of the medial temporal lobe memory system.

1 | Introduction

The perirhinal and parahippocampal cortices are key components of the medial temporal lobe memory system and play essential roles in several mnemonic and perceptual functions (Barense and Lee 2021; Lavenex and Amaral 2000; Murray and Richmond 2001; Squire and Zola 1996; Suzuki and Naya 2014). They provide the major sources of cortical input to the entorhinal cortex (Insausti, Amaral, and Cowan 1987; Suzuki and Amaral 1994b) and constitute the main conduit for information processed by the hippocampal formation to be sent back to the neocortex (Lavenex, Suzuki, and Amaral 2002). Moreover, the perirhinal

Submitted to: The Journal of Comparative Neurology

and parahippocampal cortices possess an important network of intrinsic, associational connections that participates in the integration of information before it is transmitted to the entorhinal cortex (Lavenex and Amaral 2000; Lavenex, Suzuki, and Amaral 2004). These two cortices receive and process different types of information, with the parahippocampal cortex processing mainly visuospatial information and the perirhinal cortex processing information about visual objects and emotions (Suzuki and Amaral 1994a, 1994b). Given their specific roles in mnemonic and perceptual functions, the perirhinal and parahippocampal cortices have been extensively studied in animal models, especially in rats and monkeys. However, although the general connectivity patterns and the anatomical organization of the perirhinal and parahippocampal (i.e., postrhinal in rodents) cortices are conserved across species, clear differences exist regarding some of their structural characteristics (Burwell, Witter, and Amaral 1995; Suzuki and Amaral 2003b). It is therefore important to obtain reliable quantitative estimates of the basic neuroanatomical characteristics of the perirhinal and parahippocampal cortices in these different species in order to extrapolate the experimental findings obtained in animal studies and create realistic models of the fundamental principles of human brain functions.

1.1 | Subdivisions of the Perirhinal and Parahippocampal Cortices

Combining findings from tract-tracing studies (Lavenex, Suzuki, and Amaral 2002; Lavenex, Suzuki, and Amaral 2004; Stefanacci, Suzuki, and Amaral 1996; Suzuki and Amaral 1990, 1994a, 1994b) and cyto- and chemo-architectonic analyses, Suzuki and Amaral (2003a) provided reliable definitions of the different subdivisions of the monkey perirhinal and parahippocampal cortices. We used the same definitions and criteria to delineate these regions in the present study and refer the reader to the original article for a detailed description. Briefly, the perirhinal cortex forms a band of cortex situated on the lateral bank of the rhinal sulcus and consists of a smaller medially situated area 35 and a larger laterally situated area 36 (Figure 1A–F). Area 36 can be further subdivided into rostromedial (36rm), rostrolateral (36rl), caudomedial (36cm), and caudolateral (36cl) portions. Another area, 36d, located in the dorsomedial portion of the temporal pole, is also considered part of the perirhinal cortex (Suzuki and Amaral 2003a, 2003b), although its unique anatomical and connectional characteristics set it apart from other subdivisions (Lavenex, Suzuki, and Amaral 2004). The parahippocampal cortex is caudally adjacent to the perirhinal cortex and consists of a smaller, medially situated area TH and a larger laterally situated area TF (Figure 1E–H), which can be further subdivided into a medially located area TFm (or TL following the nomenclature of Blatt, Pandya, and Rosene 2003) and a laterally adjacent area TFl. For the present study, we chose to consider areas 35, 36r (including 36rm and 36rl), and 36c (including 36cm and 36cl) for the perirhinal cortex, and areas TF (including TFm and TFl) and TH for the parahippocampal cortex, which can be reliably defined to enable stereological analyses of neuron numbers.

In humans, the perirhinal cortex is also rostrally adjacent to the parahippocampal cortex, and both are situated along the collateral and occipitotemporal sulci, although their precise location is highly dependent upon the sulcal pattern (Ding and Van Hoesen 2010; Insausti et al. 1998; Pruessner et al. 2002). The defining cytoarchitectonic features of human areas 35 and 36 of the perirhinal cortex and areas TH and TF of the parahippocampal cortex are similar to the characteristics described in monkeys (Blaizot et al. 2010; Ding and Van Hoesen 2010; Ding et al. 2009; Thangavel, Van Hoesen, and Zaheer 2008; Von Bonin and Bailey 1947; Von Economo and Koskinas 1929). Interestingly, area 35 of the human perirhinal cortex exhibits important mediolateral differences, leading researchers to divide it into distinct regions, first defined as distinct transenthorinal areas (Braak and Braak 1985) and later considered areas 35a and 35b (Augustinack et al. 2013; Ding and Van Hoesen 2010; Ding et al. 2009).

In rats, the perirhinal cortex is situated along the third quarter of the rhinal sulcus, adjacent to the entorhinal cortex, and comprises areas 35 and 36, the features of which are also remarkably similar to the corresponding areas in primates (Burwell 2001; Burwell, Witter, and Amaral 1995). Burwell et al. defined dorsal and ventral subdivisions for area 35 (35d and 35v), as well as dorsal, ventral, and posterior subdivisions for area 36 (36d, 36v, and 36p). The rodent postrhinal cortex is homologous to the primate parahippocampal cortex, based on their similar connectional, topological, and cytoarchitectural characteristics (Burwell 2001; Burwell and Amaral 1998; Burwell, Witter, and Amaral 1995). It is located caudal to area 36 and dorsal to the rhinal sulcus. The postrhinal cortex comprises a ventral and a dorsal portion (PORv and PORd), which may correspond to areas TH and TF of the monkey parahippocampal cortex, respectively (Burwell 2001; Burwell, Witter, and Amaral 1995; Furtak et al. 2007).

1.2 | Different Functional Circuits

The functional organization of the monkey perirhinal and parahippocampal cortices is characterized by their prominent interconnections with a variety of unimodal and polymodal association cortices in the temporal, frontal, and parietal lobes, as well as their close interaction with adjacent structures in the medial temporal lobe, in particular the entorhinal cortex (Amaral and Lavenex 2007). Interestingly, the perirhinal cortex and the parahippocampal cortex exhibit different patterns of connectivity with these different regions, suggesting that they contribute to different functional circuits.

Most neocortical projections reaching the perirhinal and parahippocampal cortices terminate preferentially in the superficial layers, which themselves give rise to feedforward projections toward the entorhinal cortex. In contrast, projections from the perirhinal and parahippocampal cortices toward neocortical areas originate from the deep layers and correspond to feedback-type projections typically observed in cortical areas (Felleman and Van Essen 1991; Lavenex, Suzuki, and Amaral 2002). The vast majority of cortical inputs toward the perirhinal and parahippocampal cortices come from visual areas TE, TEO, and V4 (Suzuki and Amaral 1994a). However, different types of visual information reach each of these cortices. Visual object information from area TE and rostral TEO reaches predominantly the perirhinal cortex, whereas visuospatial information from area V4, caudal TEO, and the posterior parietal cortex is directed more specifically to the parahippocampal cortex. Cortices associated with somatosensory

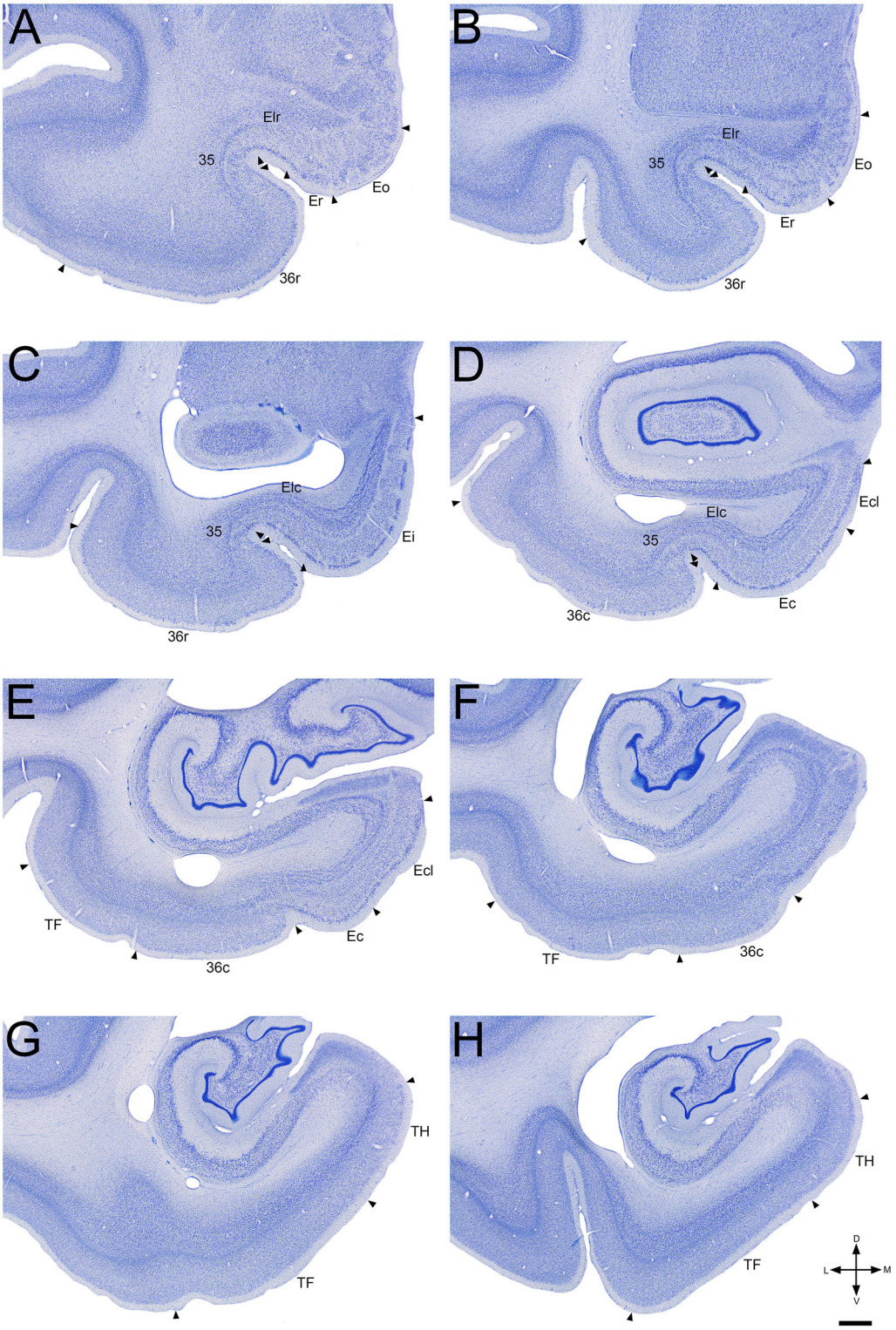

FIGURE 1 | Low-magnification photomicrographs of Nissl-stained coronal sections through the adult rhesus monkey perirhinal and parahippocampal cortices. Scale bar = 1 mm, applies to all panels. Panel (A)–(H) goes from rostral to caudal.

processing project to both the perirhinal and parahippocampal cortices, but the auditory association cortex projects mainly to the parahippocampal cortex. Both the perirhinal and parahippocampal cortices receive inputs from the superior temporal sulcus, the ventrolateral, orbitofrontal, and cingulate cortices, but the parahippocampal cortex also receives strong projections from the retrosplenial cortex. These different patterns of cortical inputs suggest that the parahippocampal cortex processes mainly visuospatial information, whereas the perirhinal cortex processes information about visual objects (Miyashita 2019). Moreover, the perirhinal cortex receives substantial projections from the lateral, basal, and accessory basal nuclei of the amygdala, whereas

the parahippocampal cortex receives only limited projections from the basal nucleus (Stefanacci, Suzuki, and Amaral 1996), suggesting a greater contribution of the perirhinal cortex to the emotional regulation of memory.

The perirhinal and parahippocampal cortices provide about two-thirds of the cortical inputs to the entorhinal cortex (Insausti, Amaral, and Cowan 1987; Suzuki and Amaral 1994b). The projections of the perirhinal and parahippocampal cortices toward the entorhinal cortex originate predominantly in layer III and terminate in the superficial layers I–III. Consistent with the view that they contribute to different functional circuits, projections from the perirhinal and parahippocampal cortices reach different subdivisions of the entorhinal cortex. The perirhinal cortex projects mainly toward the rostral portion of the entorhinal cortex (areas Eo, Er, Elr, Ei), whereas the parahippocampal cortex projects mainly toward the caudal portion of the entorhinal cortex (areas Ei, Elc, Ec, Ecl). Moreover, the rostral perirhinal cortex sends substantial projections to the lateral, basal, and accessory basal nuclei of the amygdala and the periamygdaloid cortex, whereas area TF of the parahippocampal cortex sends fewer projections to the basal and lateral nuclei (Stefanacci, Suzuki, and Amaral 1996). Both the perirhinal and parahippocampal cortices send projections to the CA1 region of the hippocampus and the subiculum, but the parahippocampal cortex also sends projections to the presubiculum (Suzuki and Amaral 1990; Van Hoesen, Rosene, and Mesulam 1979).

The feedback projections from the entorhinal cortex to the perirhinal and parahippocampal cortices follow the same topographical organization as the feedforward projections (Suzuki and Amaral 1994b). The rostral entorhinal cortex projects mainly to the perirhinal cortex, whereas the caudal entorhinal cortex projects mainly to the parahippocampal cortex. With respect to feedback projections from the perirhinal and parahippocampal cortices toward the neocortex, it is interesting to note that the parahippocampal cortex has largely reciprocal connections with the neocortex, whereas the perirhinal cortex has more asymmetric connections (Lavenex, Suzuki, and Amaral 2002). For example, the perirhinal cortex projects to more restricted regions of the frontal cortex and superior temporal sulcus than from which it receives inputs. In contrast, it projects to a larger portion of areas TE and TEO than from which it receives inputs (Lavenex, Suzuki, and Amaral 2002). This suggests that although the perirhinal and parahippocampal cortices are considered at a similar hierarchical level of the neocortical–hippocampal loop, they might also play different roles in memory consolidation processes that necessitate different types of feedback projections to the neocortex.

The overall connectivity patterns of the perirhinal and parahippocampal–postrhinal cortices are well preserved across species, although some subtle differences may exist between non-human primates and humans in the interconnections between the neocortex and the medial temporal lobe (Reznik et al. 2023). In humans, the perirhinal cortex shows preferential functional connectivity with the anterolateral entorhinal cortex (alEC or LEC), which is more responsive to pictures of objects. In contrast, the parahippocampal cortex is preferentially connected with the posteromedial entorhinal cortex (pmEC or MEC), which is more responsive to spatial scenes (Maass et al. 2015; Navarro Schroder et al. 2015). Note that on the basis of the connectivity patterns established in monkeys and the topographical organization described in monkeys and humans, the human alEC likely comprises the fields Eo, Er, Elr, and Elc and a portion of Ei, whereas pmEC comprises a portion of Ei and the fields Emi, Ec, and Ecl (Piguet et al. 2018). In rodents, the postrhinal cortex mainly interacts with the medial entorhinal cortex (MEC, homologous to the caudal entorhinal cortex in monkeys) involved in the processing of the spatial context of an experience, whereas the perirhinal cortex mainly interacts with the lateral entorhinal cortex (LEC, homologous to the rostral entorhinal cortex in monkeys) involved in the processing of the content of an experience (reviewed in Knierim, Neunuebel, and Deshmukh 2014). Accordingly, the rat postrhinal cortex shares strong anatomical connections with cortical regions associated with visuospatial processing, whereas the perirhinal cortex shares strong connections with cortical regions associated with all types of sensory modalities (Agster and Burwell 2009; Burwell and Amaral 1998).

In sum, the different patterns of connectivity of the perirhinal and parahippocampal cortices suggest a relative segregation of two functional circuits reaching the hippocampal formation: one comprising the perirhinal cortex, the rostral entorhinal cortex, and the amygdala involved in the processing of visual objects and the emotional regulation of memory, and one comprising the parahippocampal cortex, the caudal entorhinal cortex, and the presubiculum involved in the processing of spatial information and contextual memory.

1.3 | Aim of the Current Study

Despite their essential roles in mnemonic and perceptual functions, there is limited quantitative information regarding the structural characteristics of the perirhinal and parahippocampal cortices, including reliable estimates of the number and size of neurons in their different layers and subdivisions. The aim of the current study was to provide these normative data for the rhesus monkey (*Macaca mulatta*), as we have previously done for the hippocampal formation (Jabès et al. 2010, 2011), the amygdala (Chareyron et al. 2011), and the entorhinal cortex (Piguet et al. 2018). We implemented design-based stereological techniques to provide estimates of neuron number, neuronal soma size, and volume of the different layers and subdivisions of the perirhinal and parahippocampal cortices of young adult macaque monkeys (5–9 years of age). We further compared our findings with published data for rats and humans to provide a perspective on the structural organization of these brain regions in two model organisms widely used to decipher the fundamental principles of medial temporal lobe functions in humans.

2 | Materials and Methods

2.1 | Experimental Animals

Four rhesus monkeys (*M. mulatta*; two males: 5.3 and 9.4 years of age; two females: 7.7 and 9.3 years of age) were used for this study. Monkeys were born from multiparous mothers and raised at the California National Primate Research Center

(RRID:SCR_000696). They were maternally reared in 2000 m^2 outdoor enclosures and lived in large social groups until they were killed. These monkeys were some of the same animals used in quantitative studies of the monkey hippocampal formation (Jabès et al. 2010, 2011), amygdala (Chareyron, Amaral, and Lavenex 2016; Chareyron et al. 2011, 2012, 2021), entorhinal cortex (Piguet et al. 2018, 2020; Villard et al. 2023), and perirhinal cortex (Villard et al. 2023). All experimental procedures were approved by the Institutional Animal Care and Use Committee of the University of California, Davis.

2.2 | Histological Processing

2.2.1 | Brain Acquisition

Monkeys were deeply anesthetized with an intravenous injection of sodium pentobarbital (50 mg/kg i.v.; Fatal-Plus; Vortech Pharmaceuticals, Dearborn, MI, USA) and perfused transcardially with 1% and then 4% paraformaldehyde in 0.1 M phosphate buffer (PB; pH 7.4) following protocols previously described (Lavenex et al. 2009). Serial coronal sections were cut with a freezing microtome in sets of seven sections, where the first six sections were 30-μm thick and the seventh section was 60-μm thick (Microm HM 450, Microm International GmbH, Walldorf, Baden-Württemberg, Germany). The 60-μm sections were collected in 10% formaldehyde solution in 0.1 M PB (pH 7.4) and postfixed at 4°C for 4 weeks prior to Nissl staining with thionin. All other series were collected in tissue collection solution (TCS) and kept at −70°C until further processing.

2.2.2 | Nissl Staining With Thionin

The procedure for Nissl-stained sections followed our standard laboratory protocol described previously (Lavenex et al. 2009). Sections were taken out of the 10% formaldehyde solution, thoroughly washed 2 × 2 h in 0.1 M PB, mounted on gelatin-coated slides from filtered 0.05 M PB (pH 7.4), and air-dried overnight at 37°C. Sections were then defatted 2 × 2 h in a mixture of chloroform/ethanol (1:1, vol.) and rinsed 2 × 2 min in 100% ethanol, 2 min in 95% ethanol, and air-dried overnight at 37°C. Sections were then rehydrated through a graded series of ethanol, 2 min in 95% ethanol, 2 min in 70% ethanol, 2 min in 50% ethanol, dipped in two separate baths of dH_2O, and stained 20 s in a 0.25% thionin (Fisher Scientific, Waltham, MA, USA, cat# T-409) solution, dipped in two separate baths of dH_2O, 4 min in 50% ethanol, 4 min in 70% ethanol, 4 min in 95% ethanol + glacial acetic acid (1 drop per 100 mL of ethanol), 4 min in 95% ethanol, 2 × 4 min in 100% ethanol, 3 × 4 min in xylene, and coverslipped with the mounting medium DPX (BDH Laboratories, Poole, UK).

2.3 | Stereological Analyses

2.3.1 | Neuron Number

The number of mature neurons in the different layers (II–VI) of the distinct subdivisions of the perirhinal (35, 36r, 36c) and parahippocampal (TH, TF) cortices was determined using the optical fractionator method on the Nissl-stained sections cut at 60 μm (West, Slomianka, and Gundersen 1991). We estimated neuron numbers using the following formula: $N = \sum Q \times 1/\text{ssf} \times 1/\text{asf} \times 1/\text{tsf}$ (ssf: section sampling fraction; asf: area sampling fraction; tsf: thickness sampling fraction). This design-based method uses systematic random sampling and provides an estimation of the absolute number of neurons that is independent of the volume. About 16 sections (960 μm apart) per animal were used for these analyses, with the first section selected randomly within the first two sections, through which area 35 was clearly identifiable around the rhinal sulcus, corresponding approximatively to the most rostral portion of the entorhinal cortex visible on coronal sections. Note that this rostral border is a little more restrictive than in previous studies (Lavenex, Suzuki, and Amaral 2004; Suzuki and Amaral 1994a) but was considered more reliable for the stereological analyses with respect to the plane of cutting. Neuron number was estimated in the right hemisphere for half of the animals and in the left hemisphere for the other half. We used a 100× Plan Fluor oil objective (N.A. 1.30) on a Nikon Eclipse 80i microscope (Nikon Instruments Inc., Melville, NY, USA) linked to PC-based Stereo Investigator 2019 (RRID:SCR_002526; MBF Bioscience, Williston, VT, USA). Sampling schemes were established to obtain individual estimates of neuron number with coefficients of error (CE) around 0.15 using the following equation:

$$\text{CE} = \sqrt{\left(\frac{(3(A - S^2) - 4B + C)/12 + S^2}{\Sigma Q_i}\right)^2 + \left(\frac{stdev\ thickness}{mean\ thickness}\right)^2}$$

where S^2 is the variance due to noise, formerly the nugget, and

$$A = \Sigma Q_i^2 \quad B = \Sigma Q_i Q_{i+1} \quad C = \Sigma Q_i Q_{i+2}.$$

The first term of the equation corresponds to the coefficient of variation of neuron number typically used in stereological studies (for further information, see https://www.stereology.info/some-ce-theory/; Basler et al. 2017; Gundersen and Jensen 1987; Gundersen et al. 1999) to which a coefficient of error for the variation of section thickness is added. In general, the latter is not included in the basic calculations and inevitably leads to overall higher theoretical CEs (around 0.15 in the present study), but it is an important factor to consider as the estimates of neuron number are highly dependent on the section thickness (for more information, see Peruzzi 2012). Note that empirical CEs based on true replicates of neuron number estimates are typically lower than the theoretical CEs calculated from these formulas (data not shown).

Details of the stereological sampling schemes are described in Table 1. A disector of 5 μm was chosen to ensure that the same stereological parameters could be used in a follow-up study on the development of these structures. An average of one neuron was counted per disector, in line with recommended standards (Slomianka 2021). Neurons were counted when their nucleolus (or nucleus if there were more than one nucleolus) came into focus within the counting frame, as it was moved through a known distance of the section thickness. We identified neurons based on morphological criteria identifiable in Nissl preparations, as previously described (Chareyron, Amaral, and Lavenex 2016; Chareyron et al. 2012; García-Cabezas et al. 2016; Piguet et al. 2018). García-Cabezas et al. (2016) provided a particularly well-illustrated and detailed description of the cytology of Nissl-stained neurons, glial cells, and endothelial

TABLE 1 | Parameters used for the stereological analysis of the rhesus monkey perirhinal and parahippocampal cortices.

Area	Layer	Number of sections	Distance between sections (μm)	Scan grid (μm)[a]	Counting frame (μm)	Disector height (μm)	Guard zones (μm)	Average section thickness[b]	Number of neurons counted (range)	Number of disectors (range)	Coefficients of error (CE)
35	II	7–8	960	100 × 100	40 × 40	5	2	14.11 (12.7–15.3)	145 (130–178)	130 (117–148)	0.14 (0.12–0.15)
	III	7–8	960	150 × 150	40 × 40	5	2	14.70 (13.5–15.8)	120 (100–138)	107 (95–120)	0.15 (0.11–0.18)
	V	7–8	960	150 × 150	40 × 40	5	2	14.33 (13.4–15.3)	132 (114–145)	107 (103–112)	0.15 (0.10–0.17)
	VI	7–8	960	200 × 200	40 × 40	5	2	13.59 (13.1–15.5)	131 (119–147)	114 (106–131)	0.14 (0.11–0.16)
36r	II	6	960	200 × 200	20 × 20	5	2	12.24 (11.5–12.9)	198 (176–216)	288 (254–328)	0.13 (0.12–0.13)
	III	6	960	400 × 400	30 × 30	5	2	13.13 (12.3–14.2)	141 (109–182)	149 (121–190)	0.15 (0.12–0.16)
	IV	6	960	200 × 200	20 × 20	5	2	13.57 (12.7–14.9)	132 (123–143)	136 (101–157)	0.14 (0.11–0.17)
	V	6	960	300 × 300	30 × 30	5	2	13.30 (12.7–14.3)	160 (127–192)	146 (114–188)	0.13 (0.10–0.15)
	VI	6	960	250 × 250	30 × 30	5	2	13.11 (12.4–14.2)	129 (99–151)	158 (121–203)	0.14 (0.12–0.17)
36c	II	4–5	960	200 × 200	20 × 20	5	2	12.86 (12.0–13.0)	109 (91–132)	153 (118–215)	0.18 (0.15–0.25)
	III	4–5	960	300 × 300	30 × 30	5	2	13.89 (12.8–14.7)	128 (98–146)	128 (88–167)	0.17 (0.15–0.20)
	IV	4–5	960	150 × 150	20 × 20	5	2	14.36 (13.0–15.4)	124 (95–166)	128 (99–177)	0.15 (0.15–0.17)
	V	4–5	960	230 × 230	30 × 30	5	2	14.29 (13.4–15.1)	165 (99–197)	154 (93–205)	0.15 (0.14–0.17)
	VI	4–5	960	200 × 200	30 × 30	5	2	14.20 (13.4–15.0)	123 (103–137)	145 (105–184)	0.15 (0.13–0.16)
TH	II	4–5	960	170 × 170	30 × 30	5	2	13.53 (13.4–15.2)	194 (157–227)	119 (113–125)	0.17 (0.09–0.26)
	III	4–5	960	270 × 270	30 × 30	5	2	14.26 (13.1–16.0)	153 (128–165)	109 (92–123)	0.15 (0.10–0.22)
	V	4–5	960	230 × 230	30 × 30	5	2	14.60 (13.8–16.1)	129 (104–156)	88 (76–104)	0.15 (0.13–0.16)
	VI	4–5	960	150 × 150	30 × 30	5	2	14.57 (13.6–15.7)	115 (82–135)	122 (96–139)	0.13 (0.10–0.17)
TF	II	9	960	320 × 320	20 × 20	5	2	13.84 (13.1–15.1)	113 (98–130)	127 (111–159)	0.17 (0.14–0.22)
	III	9	960	550 × 550	30 × 30	5	2	15.05 (14.5–16.9)	104 (93–110)	88 (73–111)	0.16 (0.11–0.20)
	IV	9	960	220 × 220	20 × 20	5	2	15.25 (14.1–16.8)	160 (132–198)	145 (112–183)	0.14 (0.12–0.16)
	V	9	960	430 × 430	30 × 30	5	2	15.12 (14.1–16.4)	139 (117–167)	108 (90–139)	0.13 (0.11,0.15)
	VI	9	960	330 × 330	30 × 30	5	2	14.84 (14.3–16.0)	102 (98–124)	108 (90–124)	0.13 (0.11–0.14)

[a]Scan grid was placed in a random orientation.

[b]Section thickness was measured at every other counting site.

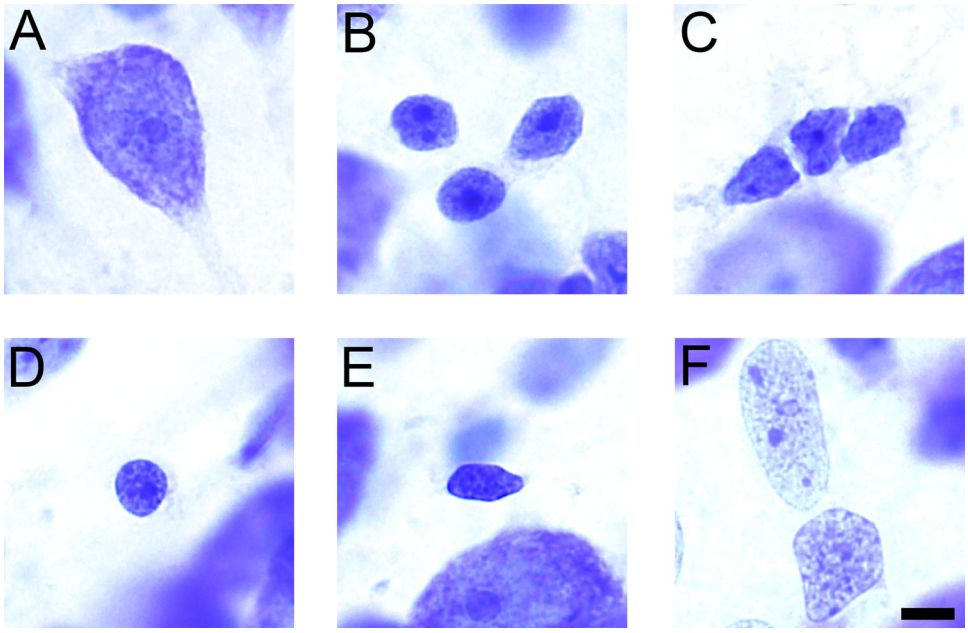

FIGURE 2 | Classification and identification of different cell types in the monkey perirhinal and parahippocampal cortices, viewed with a ×100 objective in Nissl-stained sections: (A) neuron; (B) immature neurons; (C) astrocytes; (D) oligodendrocyte; (E) microglia; (F) endothelial cells. Scale bar = 5 μm, applies to all panels.

cells. Briefly, neurons are darkly stained, always have visible cytoplasm around their nucleus, and usually comprise a single large nucleolus (Figure 2A). Immature neurons, as described in Chareyron, Amaral, and Lavenex (2016), which are present in the monkey perirhinal cortex (Villard et al. 2023) but were not quantified in the current study, have a round to slightly oval, hyperchromatic nucleus containing distinguishable nucleoli (Figure 2B). Astrocytes are more irregularly shaped than neurons and exhibit a relatively paler staining of the nucleus with an occasional rim of lightly stained cytoplasm (Figure 2C). Oligodendrocytes are smaller than astrocytes and contain a round, smooth, darkly stained nucleus that is densely packed with chromatin (Figure 2D). Microglia have the smallest nucleus, dark staining, and an irregular shape that is often rodlike, oval, or bent (Figure 2E). Endothelial cells exhibit a lightly stained and flat nucleus that molds to the tubular shape of capillaries (Figure 2F).

2.3.2 | Volume Estimates

We estimated the volume of the individual layers of each subdivision of the monkey perirhinal and parahippocampal cortex based on the outline tracings performed with Stereo Investigator 2019 for the estimation of neuron numbers. We used the section cutting thickness (60 μm) to determine the distance between sampled sections, which was then multiplied by the total surface area delineated for neuron counts to calculate the volume.

2.3.3 | Neuronal Soma Size

The volume of the soma of every neuron counted during the optical fractionator analysis was determined using the nucleator method (Gundersen 1988). The nucleator is used to estimate the mean cross-sectional area and volume of cells. A set of three rays emanating from a randomly chosen point within the nucleus or nucleolus is drawn and oriented randomly. The lengths of the intercepts from the point to the cell boundary (l) are measured, and the cell volume is obtained by calculating the mean of $V = (4/3 \times 3.1416) \times l^3$. Essentially, this is the formula used to determine the volume of a sphere with a known radius. We measured an average of 137 neurons per layer per subdivision (Table 1). Note that the nucleator method provides accurate estimates of neuron size when isotropic-uniform-random sectioning of brain structures is employed. In our study, all brains were cut in the coronal plane. Estimates of cell size might therefore be impacted by the nonrandom orientation of neurons in the different layers and subdivisions of the perirhinal and parahippocampal cortices, which could lead to an overestimation or underestimation of cell size in any given structure.

2.3.4 | Statistical Analyses

We used SPSS (RRID:SCR_002865) to perform general linear model analyses with subdivisions of the perirhinal cortex (35, 36r, 36c) or parahippocampal cortex (TF, TH) as repeated measures. Post hoc analyses were performed with the Fisher least significant difference test when the ANOVA F ratio was significant. Significance level was set at $p < 0.05$ for all analyses. We reported effect size with partial eta squared (η^2).

2.3.5 | Photomicrographic Production

Low-magnification photomicrographs were taken with a Leica DFC420 digital camera on a Leica MZ9.5 stereomicroscope (Leica Microsystems GmbH, 35578 Wetzlar, Germany). Artifacts located outside the sections were removed, and color balance was

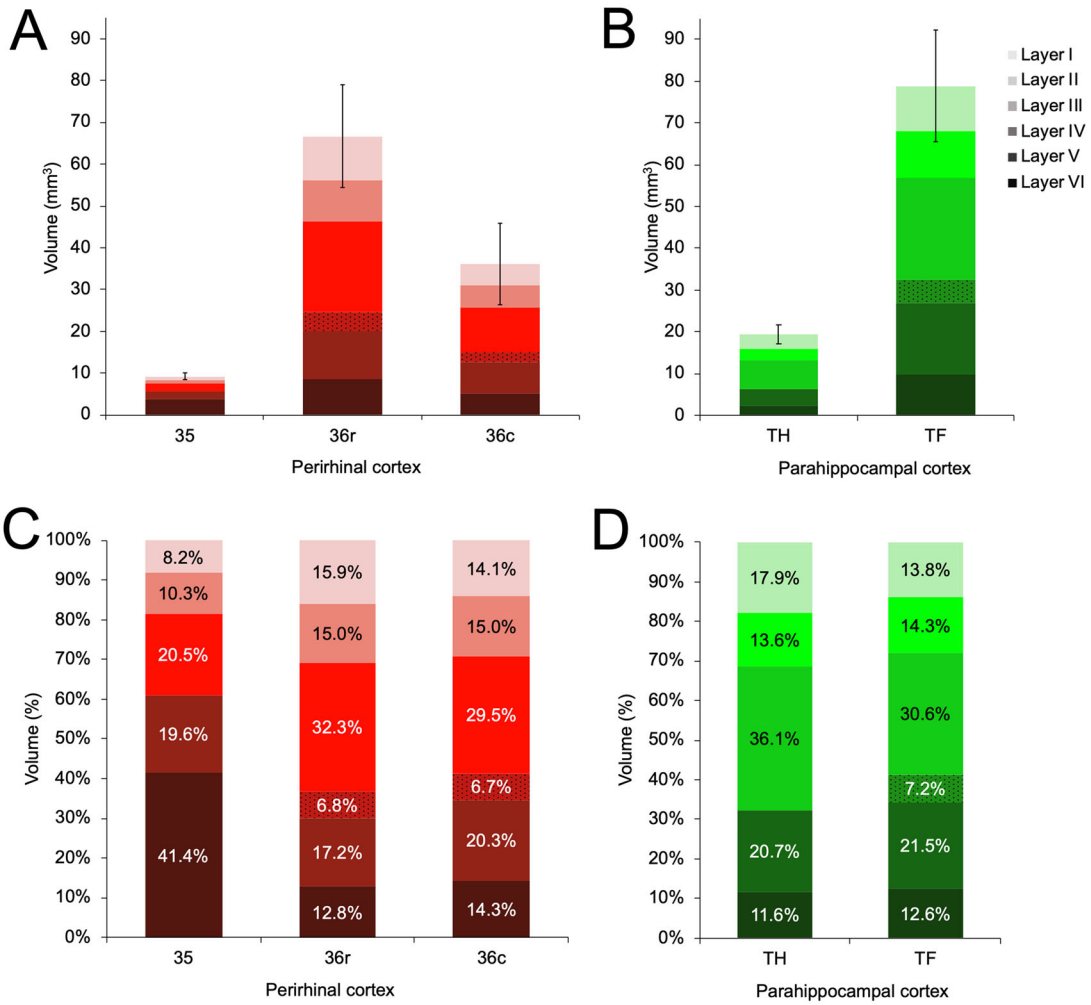

FIGURE 3 | (A and B) Volumes of the different layers of areas 35, 36r, and 36c of the perirhinal cortex, and areas TH and TF of the parahippocampal cortex; (C and D) Percentages of the volume occupied by each layer, per subdivision.

adjusted in Adobe Photoshop V 24.0.1 (RRID:SCR_014199 Adobe Systems, San Jose, CA, USA) to improve contrast and clarity.

3 | Results

3.1 | Volumes of the Different Layers and Subdivisions

The volumes of the different layers of the distinct subdivisions of the perirhinal and parahippocampal cortices are presented in Table 2 and Figure 3.

3.1.1 | Perirhinal Cortex

Area 35 represents about 8% of the volume of the entire perirhinal cortex (excluding 36d), area 36r 60%, and area 36c 32%. The relative volume of individual layers is similar in areas 36r and 36c. Their superficial layers I–III together account for about 62% of the entire volume of area 36 (including 36r and 36c); layer III is the largest, accounting for about 31%, and layers I and II for about 15% each. Layer IV represents only about 7% of area 36. There is no layer IV in area 35. The deep layers V and VI together represent about one-third of the entire volume of area 36, with layer V accounting for about 18% and layer VI for about 13%. Interestingly, the superficial and deep layers of area 35 exhibit opposite proportions. The deep layers V and VI of area 35 account for about 61% of its entire volume, with layer V accounting for about 20% and layer VI for about 41%. The superficial layers I–III represent about 39% of the volume of area 35.

3.1.2 | Parahippocampal Cortex

Area TH represents 20% of the entire volume of the parahippocampal cortex and area TF 80%. Similar to areas 36r and 36c of the perirhinal cortex, the superficial layers I–III of areas TH and TF account together for about 61% of the entire volume of the parahippocampal cortex; layer III is the largest, accounting for about 32%, and layers I and II for about 15% and 14%, respectively. Layer IV represents only 7% of the volume of area TF. There is no layer IV in area TH. The deep layers V and VI of areas TH and TF represent about one-third of the entire volume of the parahippocampal cortex, with layer V accounting for about 21% and layer VI for about 12%.

TABLE 2 | Volume, neuron number, and neuron soma size in the different layers of the distinct subdivisions of the rhesus monkey perirhinal and parahippocampal cortices.

		Volume (mm^3)			Neuron number			Neuron soma size (μm^3)	
		Mean	**SD**	**%**	**Mean**	**SD**	**%**	**Mean**	**SD**
35	I	0.75	0.10	8.2	—	—	—	—	—
	II	0.95	0.11	10.3	40,922	6,366	11.8	1,966	170
	III	1.88	0.22	20.5	78,648	9,447	22.7	1,844	223
	V	1.80	0.07	19.6	84,795	7,801	24.5	1,988	172
	VI	3.81	0.39	41.4	142,569	16,447	41.1	1,597	196
	Total[a]	9.19	0.78	100.0	346,934	34,303	100.0	—	—
36r	I	10.48	1.25	15.9	—	—	—	—	—
	II	9.91	1.36	15.0	775,309	99,867	22.5	1,404	44
	III	21.66	5.06	32.3	1,065,249	300,898	30.3	1,546	96
	IV	4.47	0.72	6.8	571,951	69,981	16.6	777	85
	V	11.49	2.73	17.2	684,818	134,940	19.8	1,654	156
	VI	8.61	1.98	12.8	382,282	84,649	10.9	1,549	71
	Total[a]	66.62	12.33	100.0	3,479,609	628,045	100.0	—	—
36c	I	5.02	1.01	14.1	—	—	—	—	—
	II	5.37	1.34	15.0	448,180	81,400	22.3	1,378	58
	III	10.71	3.09	29.5	571,904	129,130	28.1	1,534	107
	IV	2.42	0.68	6.7	322,541	98,295	15.7	716	82
	V	7.44	2.42	20.3	446,022	132,723	21.7	1,564	158
	VI	5.16	1.38	14.3	249,957	60,458	12.3	1,420	92
	Total[a]	36.12	9.75	100.0	2,038,604	476,416	100.0	—	—
Perirhinal	I	16.25	2.32	14.7	—	—	—	—	—
	II	16.23	2.73	14.6	1,264,411	179,273	21.7	1,582	62
	III	34.25	7.98	30.5	1,715,801	406,328	29.1	1,641	109
	IV	6.89	1.23	6.2	894,492	164,162	15.3	746	27
	V	20.73	5.05	18.4	1,215,635	270,807	20.7	1,735	104
	VI	17.58	3.66	15.7	774,808	157,860	13.2	1,522	88
	Total[a]	111.93	22.23	100.0	5,865,147	1,109,303	100.0	1,495	58
TH	I	3.46	0.37	17.9	—	—	—	—	—
	II	2.62	0.11	13.6	267,617	38,507	20.5	1,263	166
	III	7.02	0.95	36.1	567,100	97,598	42.8	1,383	61
	V	4.04	0.68	20.7	352,391	56,769	26.7	1,738	81
	VI	2.27	0.40	11.6	133,689	26,978	10.0	1,494	74
	Total[a]	19.41	2.22	100.0	1,320,797	181,500	100.0	—	—
TF	I	10.75	1.30	13.8	—	—	—	—	—
	II	11.25	1.71	14.3	1,274,438	125,680	21.9	1,083	87
	III	24.23	4.83	30.6	1,676,232	156,773	28.7	1,233	83
	IV	5.71	1.35	7.2	942,216	185,835	16.0	586	37
	V	17.00	3.53	21.5	1,383,945	287,091	23.5	1,425	164
	VI	9.87	1.46	12.6	588,363	104,078	10.0	1,418	153
	Total[a]	78.81	13.37	100.0	5,865,194	733,304	100.0	—	—

(Continues)

TABLE 2 | (Continued)

		Volume (mm^3)			Neuron number			Neuron soma size (μm^3)	
		Mean	SD	%	Mean	SD	%	Mean	SD
Parahipp	I	14.21	1.34	14.6	—	—	—	—	—
	II	13.87	1.76	14.2	1,542,055	100,820	21.6	1,173	85
	III	31.25	5.50	31.7	2,243,332	177,467	31.3	1,308	22
	IV	5.71	1.35	5.8	942,216	185,835	13.1	586	37
	V	21.04	4.19	21.3	1,736,336	332,334	24.0	1,581	104
	VI	12.14	1.76	12.4	722,052	113,868	10.0	1,456	102
	Total[a]	98.22	14.97	100.0	7,185,991	732,814	100.0	1,291	48

[a]Totals were calculated based on the rounded data listed above.

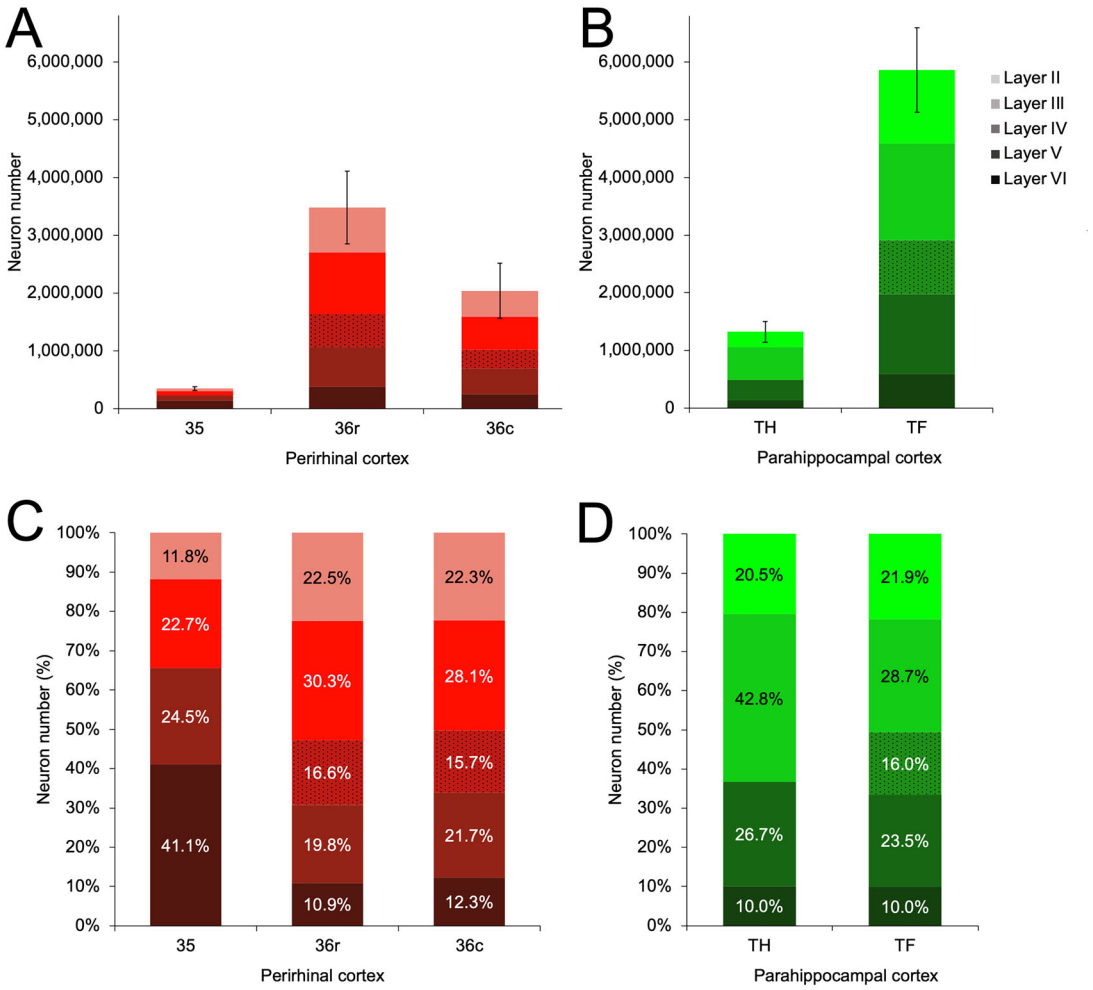

FIGURE 4 | (A and B) Numbers of neurons in the different layers of areas 35, 36r, and 36c of the perirhinal cortex, and areas TH and TF of the parahippocampal cortex; (C and D) percentages of neurons located in each layer, per subdivision.

3.2 | Neuron Numbers in Different Layers and Subdivisions

The numbers of neurons in the different layers of the distinct subdivisions of the perirhinal cortex and parahippocampal cortex are presented in Table 2 and Figure 4.

3.2.1 | Perirhinal Cortex

Consistent with the volume estimates, about 6% of all neurons of the perirhinal cortex are located in area 35, 59% in area 36r, and 35% in area 36c. The relative numbers of neurons in the different layers are similar in areas 36r and 36c. About half of the neurons

are located in the superficial layers II and III of area 36 (including 36r and 36c), which contribute the main feedforward projections to the entorhinal cortex; about 30% of neurons are located in layer III and 22% in layer II. In contrast, only one-third of neurons are located in the deep layers V and VI, which are the main recipients of the feedback projections originating in the entorhinal cortex; about 21% of neurons are located in layer V and 11% in layer VI. About 16% of neurons are located in layer IV of area 36. In contrast to other subdivisions, two-thirds of the neurons in area 35 are located in the deep layers, with 25% in layer V and 41% in layer VI. About one-third of neurons are located in the superficial layers of area 35, with 12% in layer II and 23% in layer III.

3.2.2 | Parahippocampal Cortex

About 18% of all neurons in the parahippocampal cortex are located in area TH and 82% in area TF. Similar to areas 36r and 36c of the perirhinal cortex, about half of the neurons of areas TH and TF are located in the superficial layers II and III, which contribute the main feedforward projections of the parahippocampal cortex to the entorhinal cortex. About 31% of neurons are located in layer III and 22% in layer II. In contrast, only about one-third of the neurons are located in the deep layers V and VI, which are the main recipients of the feedback projections from the entorhinal cortex. The number of neurons in layer IV of area TF represents about 16% of neurons in this subdivision, similarly to what is found in area 36.

3.2.3 | Superficial/Deep Neuron Number Ratios

In light of the variations in the number of neurons located in the superficial layers II and III and in the deep layers V and VI (which contribute and receive different input and output projections to and from the entorhinal cortex, respectively), it is interesting to compare the ratio of the number of neurons located in the superficial versus deep layers in different areas (Figure 5). The ratio was calculated by dividing the number of neurons present in the superficial layers (II and III) by the number of neurons present in the deep layers (V and VI). The ratio differed between the subdivisions of the perirhinal cortex ($F_{(2,6)} = 63.937$, $p < 0.001$, $\eta^2 = 0.955$); area 35 exhibited a lower ratio than areas 36r ($p = 0.004$) and 36c ($p = 0.002$), and area 36r tended to exhibit a slightly higher ratio than area 36c ($p = 0.070$). Similarly, in the parahippocampal cortex, the ratio between the number of neurons located in the superficial versus deep layers was slightly higher in area TH than in area TF ($F_{(2,3)} = 8.372$, $p = 0.063$, $\eta^2 = 0.736$). Across all the subdivisions of the perirhinal and parahippocampal cortices, the ratio differed ($F_{(4,12)} = 34.725$, $p < 0.001$, $\eta^2 = 0.920$); in particular, in addition to the differences just described, area 35 exhibited a much lower ratio than areas TF ($p = 0.004$) and TH ($p < 0.001$).

3.3 | Neuronal Soma Size

The average neuronal soma size in the different layers of the distinct subdivisions of the perirhinal and parahippocampal cortices are presented in Table 2 and Figure 6. Considering that, as predicted, soma size varies substantially among layers, statistical analyses were performed separately for the different layers.

3.3.1 | Layer II

The average soma volume of layer II neurons differed between subdivisions of the perirhinal cortex ($F_{(2,6)} = 39.99$, $p < 0.001$, $\eta^2 = 0.929$). Layer II neurons were larger in area 35 than in areas 36r ($p = 0.013$) and 36c ($p = 0.002$); soma size did not differ between areas 36r and area 36c ($p = 0.642$). In the parahippocampal cortex, the average soma volume of layer II neurons did not differ between areas TH and TF ($F_{(1,3)} = 3.077$, $p = 0.178$, $\eta^2 = 0.506$). Across all subdivisions ($F_{(4,12)} = 25.596$, $p < 0.001$, $\eta^2 = 0.895$), layer II neurons were larger in area 35 than in areas TH ($p = 0.022$) and TF ($p = 0.004$); layer II neurons were smaller in area TF than in areas 35 ($p = 0.004$), 36r ($p = 0.007$), and 36c ($p = 0.014$).

3.3.2 | Layer III

The average soma volume of layer III neurons differed between the subdivisions of the perirhinal cortex ($F_{(2,6)} = 7.094$, $p = 0.026$, $\eta^2 = 0.703$). Neurons in area 35 were larger than in area 36c ($p = 0.019$), but the difference did not reach statistical significance compared to neurons in area 36r ($p = 0.101$). Neuronal soma size did not differ between areas 36r and 36c ($p = 0.876$). There was no difference between the subdivisions of the parahippocampal cortex ($F_{(1,3)} = 4.711$, $p = 0.118$, $\eta^2 = 0.611$). However, when considering all subdivisions ($F_{(4,12)} = 15.283$, $p < 0.001$, $\eta^2 = 0.836$), layer III neurons were generally smaller in area TF than in the different areas of the perirhinal cortex (35, $p = 0.007$; 36r, $p = 0.032$; 36c, $p = 0.013$). Neurons in area TH were also smaller than in areas 35 ($p = 0.031$), 36r ($p = 0.007$), and 36c ($p = 0.080$).

3.3.3 | Layer IV

The average soma volume of layer IV neurons differed between areas 36r, 36c, and TF (the three areas in which this layer is present; $F_{(2,6)} = 5.184$, $p = 0.049$, $\eta^2 = 0.633$). Layer IV neurons tended to be smaller in area TF than in areas 36r ($p = 0.027$) and 36c ($p = 0.083$), whereas no difference was found between areas 36r and 36c ($p = 0.492$).

3.3.4 | Layer V

The average soma volume of layer V neurons differed between the subdivisions of the perirhinal cortex ($F_{(2,6)} = 8.611$, $p = 0.017$, $\eta^2 = 0.742$). Neurons was larger in area 35 than in areas 36r ($p = 0.042$) and 36c ($p = 0.031$), whereas soma size did not differ between areas 36r and 36c ($p = 0.488$). The average soma volume of layer V neurons were larger in area TH than in area TF ($F_{(1,3)} = 16.632$, $p = 0.027$, $\eta^2 = 0.847$). When considering all subdivisions ($F_{(4,12)} = 8.750$, $p = 0.002$, $\eta^2 = 0.745$), layer V neurons were larger in area 35 of the perirhinal cortex than in areas TH ($p = 0.053$) and TF ($p = 0.006$) of the parahippocampal cortex.

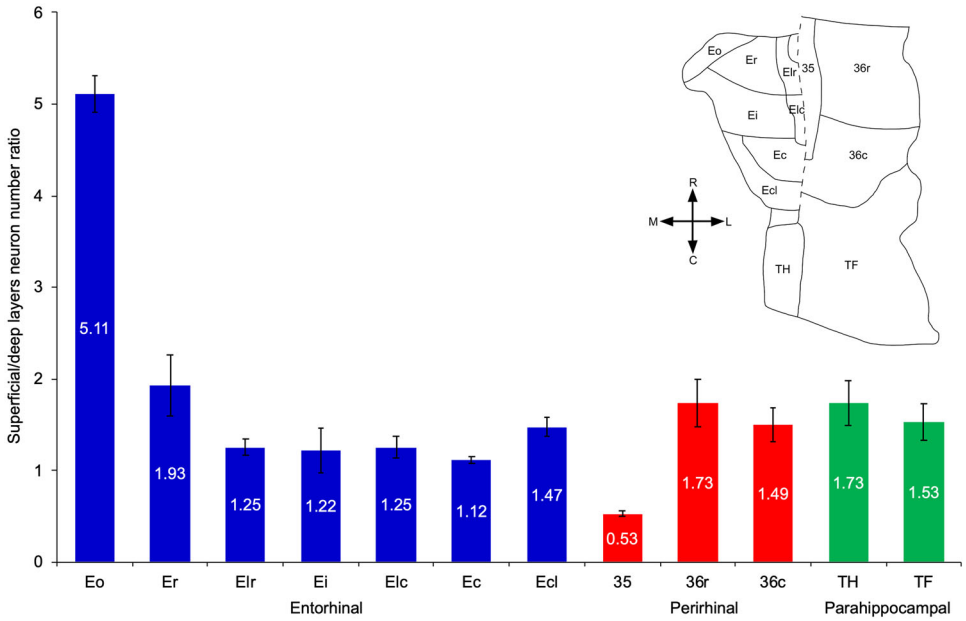

FIGURE 5 | Ratio of the number of neurons located in the superficial layers (II and III) and the number of neurons located in the deep layer (V and VI) for areas Eo, Er, Elr, Ei, Elc, Ec, and Ecl of the entorhinal cortex in blue, areas 35, 36r, and 36c of the perirhinal cortex in red, and areas TH and TF of the parahippocampal cortex in green. Ratios were calculated by dividing the number of neurons in the superficial layers by the number of neurons in the deep layers. *Source:* Data from Piguet et al. (2018) for the entorhinal cortex.

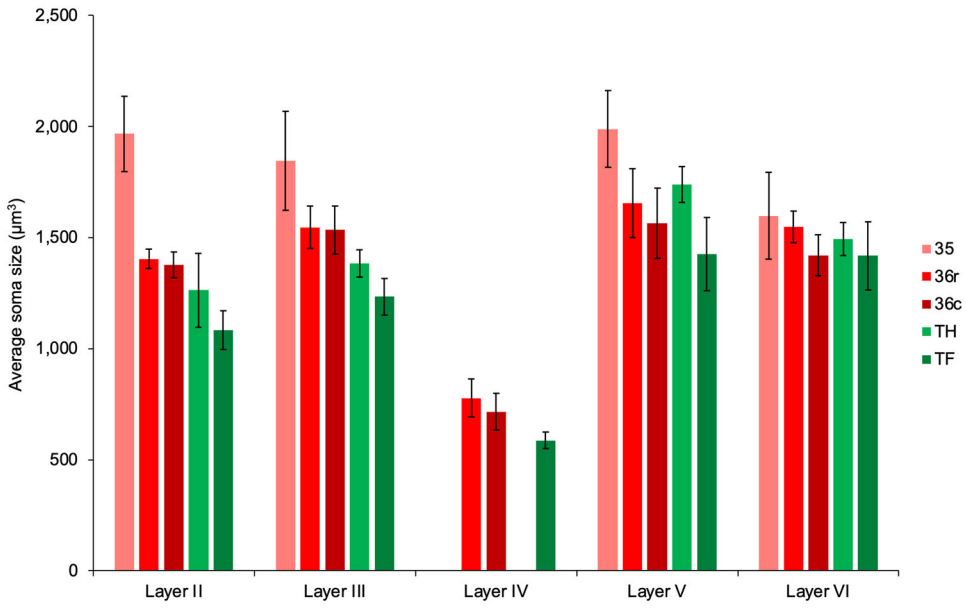

FIGURE 6 | Average neuronal soma size for each layer of areas 35, 36r, and 36c of the perirhinal cortex, and areas TH and TF of the parahippocampal cortex.

3.3.5 | Layer VI

The average soma volume of layer VI neurons did not differ between the subdivisions of the perirhinal cortex ($F_{(2,6)} = 2.340$, $p = 0.177$, $\eta^2 = 0.438$), although layer VI neurons tended to be smaller in area 36c than in area 36r ($p = 0.069$). Average neuronal soma size did not differ between the subdivisions of the parahippocampal cortex ($F_{(1,3)} = 1.448$, $p = 0.315$, $\eta^2 = 0.326$), or when considering all subdivisions ($F_{(4,12)} = 2.581$, $p = 0.091$, $\eta^2 = 0.462$).

3.3.6 | Entorhinal, Perirhinal, and Parahippocampal Cortices

Considering the general tendency for neurons to be smaller in the parahippocampal cortex than in the perirhinal cortex, we further

compared neuronal soma size in these two cortices with previously acquired data in the entorhinal cortex (Piguet et al. 2018). Overall, average neuronal soma size across all layers differed between the three cortices ($F_{(2,6)} = 188.877$, $p > 0.001$, $\eta^2 = 0.984$). As suspected based on the separate analyses performed for each layer described above, neuronal somas were overall larger in the perirhinal cortex than in the parahippocampal cortex ($p = 0.006$). Interestingly, neuronal somas were larger in the entorhinal cortex compared to both the perirhinal cortex ($p < 0.001$) and the parahippocampal cortex ($p < 0.001$). Note that these differences remained when excluding the granular layer IV, which is not present in all subdivisions and is characterized by smaller neurons ($F_{(2,6)} = 127.812$, $p < 0.001$, $\eta^2 = 0.977$; entorhinal > perirhinal, $p < 0.001$; entorhinal > parahippocampal, $p = 0.001$; perirhinal > parahippocampal, $p = 0.005$). Considering the average neuronal soma size in the different subdivisions of the perirhinal and parahippocampal cortices compared to the entorhinal cortex ($F_{(5,15)} = 74.664$, $p < 0.001$, $\eta^2 = 0.961$), neurons were smaller in area 35 than in the entorhinal cortex ($p = 0.044$), but larger than in areas 36r ($p = 0.007$), 36c ($p = 0.002$), TH ($p = 0.014$), and TF ($p < 0.001$). Average neuronal soma size did not differ between areas 36r and 36c ($p = 0.259$), but neurons in these two areas tended to be larger than neurons in areas TH (36r, $p = 0.067$; 36c, $p = 0.058$) and TF (36r, $p < 0.001$; 36c, $p = 0.022$). Average neuronal soma size was larger in area TH than in area TF ($p = 0.011$).

4 | Discussion

In this study, we provide normative data on the volume, neuron number, and neuronal soma size in the different layers and subdivisions of the adult rhesus monkey perirhinal and parahippocampal cortices. We found that areas 36r and 36c of the perirhinal cortex and areas TH and TF of the parahippocampal cortex exhibit similar laminar organizations in terms of relative volume and neuron number. They are characterized by relatively large superficial layers I–III (as compared to deep layers V and VI), which contain about half of the total number of neurons in these areas. In contrast, area 35 exhibits relatively large deep layers V and VI, which contain about two-thirds of its total number of neurons. In general, neurons are larger in the perirhinal cortex than in the parahippocampal cortex, and even larger in the entorhinal cortex. These morphological characteristics are consistent with previously described patterns of relative laminar development across different areas of the primate cerebral cortex (Barbas 1986; Barbas and Rempel-Clower 1997; Bautista et al. 2023; Garcia-Cabezas, Hacker, and Zikopoulos 2023; Hilgetag and Goulas 2020). Here, we first discuss our findings in light of the organization of cortico–cortical connections, which reflects the position of a brain region within a hierarchy of associational networks. Second, we discuss how the current findings provide corroborative information on the functional organization of medial temporal lobe circuits. Finally, we compare our findings in monkeys with those obtained in rats and humans, to provide a perspective to extrapolate findings from experimental studies in animals and create realistic models of the medial temporal lobe memory system.

4.1 | Laminar Organization and Cortical Hierarchy

One particular feature of the perirhinal and parahippocampal cortices that emerged from our study is that their superficial layers, in which originate the main feedforward projections to the entorhinal cortex (Suzuki and Amaral 1994b), represent about 60% of their entire volume and contain about half of the total number of neurons found in these areas. In monkeys, relatively large or thick superficial layers have been described in the entorhinal cortex (Piguet et al. 2018) and other multimodal associative cortices, such as area 30 of the retrosplenial cortex, areas 23 and 31 of the cingulate cortex (Zilles et al. 1986), and area 10 of the prefrontal cortex (Semendeferi et al. 2001). Interestingly, superficial layers are less thick in unimodal and primary cortices and seem to expand along the hierarchy of cortical associational networks (de Sousa et al. 2010; Sherwood et al. 2004). For example, the superficial layers II and III only account for a small proportion (28%) of the cortical thickness in the primary visual cortex (area V1). This proportion is higher in the secondary visual area V2 (42%) and even higher in the ventral posterior (VP) area (47%), which are located further up in the hierarchy of the monkey visual system (de Sousa et al. 2010; Felleman, Burkhalter, and Van Essen 1997). Accordingly, while the superficial layers I–III account for about 60% of the total volume of the perirhinal and parahippocampal cortices, these layers account for 68% of the total volume of the entorhinal cortex (Piguet et al. 2018), which is located at a higher level in the hierarchy of medial temporal lobe structures (Lavenex and Amaral 2000). The relatively larger size of the superficial layers in the perirhinal and parahippocampal cortex is thus in line with a progressive increase in the relative size of these layers along a hierarchy of cortical areas and, as such, reflects the pivotal role of these cortices as recipients and integrators of various cortical inputs to be transmitted to the entorhinal cortex.

Similarly, the morphological characteristics of layer III neurons vary across cortical areas (Elston, Benavides-Piccione, and Defelipe 2005; Elston and Rosa 1997, 1998; Garcia-Cabezas, Barbas, and Zikopoulos 2018). Along the monkey occipitotemporal visual pathway, layer III neurons show a serial increase in somal area, dendritic complexity, and spine density from V1, to V2, to V4, to TEO (Elston and Rosa 1998). Similar differences were reported in the occipitoparietal pathway from areas V1 and V2 to areas MT, LIPv, and 7a (Elston and Rosa 1997) and between the posterior and anterior cingulate cortices (Elston, Benavides-Piccione, and Defelipe 2005). Larger neurons with more complex structures are likely adapted to integrate a larger number of inputs coming from various brain regions. Consistent with such differences in neuronal morphology, neuronal density gradually decreases from primary visual areas to unimodal and polymodal areas (Hilgetag and Goulas 2020; Hilgetag et al. 2016). In the current study, we found smaller neuronal soma sizes in the perirhinal and parahippocampal cortices, as compared to the entorhinal cortex, which is at a higher level in the hierarchy of medial temporal lobe circuits (Lavenex and Amaral 2000). Interestingly, we also found smaller neuronal soma sizes in the parahippocampal cortex as compared to the perirhinal cortex. Although the two cortices are often considered to be at the same hierarchical level based on their

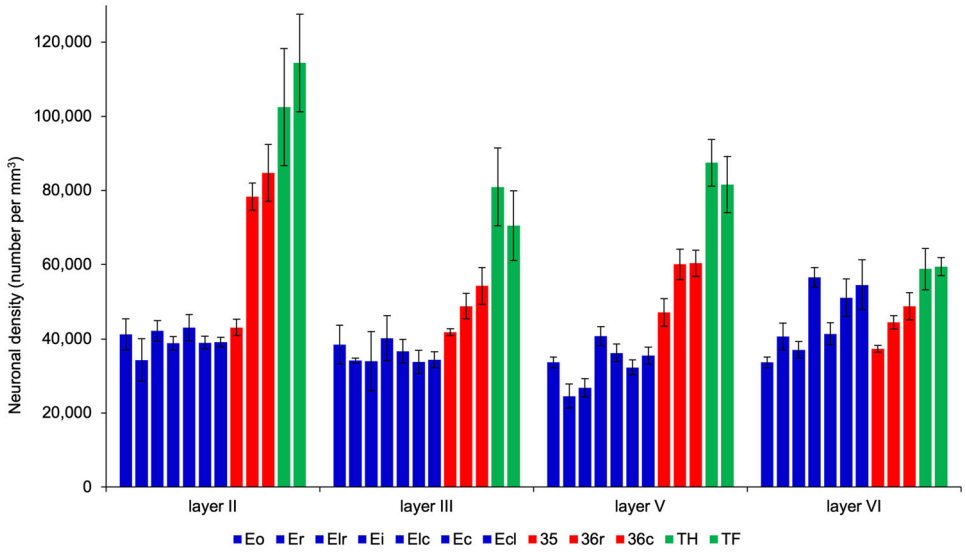

FIGURE 7 | Neuronal density (number of neurons per mm^3) for the different layers of the distinct subdivisions of the entorhinal cortex (areas Eo, Er, Elr, Ei, Elc, Ec, and Ecl), perirhinal cortex (areas 35, 36r, and 36c), and parahippocampal cortex (areas TH and TF). Neuronal density was calculated by dividing the number of neurons by the volume of a specific area. *Source:* Retrieved from Piguet et al. (2018) for the entorhinal cortex.

position between various cortical areas and the entorhinal cortex (Lavenex and Amaral 2000), the laminar organization of their interconnections (Lavenex, Suzuki, and Amaral 2004), together with these differences in neuronal soma size, suggest that the perirhinal cortex is at a higher level than the parahippocampal cortex within medial temporal lobe circuits. Accordingly, we found that the parahippocampal cortex has a higher neuronal density than the perirhinal cortex (Figure 7), as was previously reported by Hilgetag et al. (2016). Our measures of neuronal density and soma size thus corroborate previous findings and interpretation of a hierarchical organization between these two cortices.

4.2 | Medial Temporal Lobe Circuits

The perirhinal and parahippocampal cortices receive the vast majority of their cortical inputs from unimodal visual areas TE, TEO, and V4, but also from multimodal association cortices in the temporal, frontal, and parietal lobes and somatosensory cortices, suggesting a convergence of various types of information in the perirhinal and parahippocampal cortices (Suzuki and Amaral 1994a). As mentioned previously, different types of information reach the perirhinal and parahippocampal cortices, thus contributing to distinct functional circuits. Visual object information from area TE and rostral TEO reaches predominantly the perirhinal cortex, whereas visuospatial information from area V4, caudal TEO, and the posterior parietal cortex is directed more specifically to the parahippocampal cortex. Interestingly, despite the fact that the perirhinal cortex and parahippocampal cortex contribute to distinct functional circuits, the proportions of volume and neuron number located in the superficial versus deep layers are relatively similar across areas 36r, 36c, TH, and TF. These proportions may therefore be relatively independent of the type of information being processed and rather reflect fundamental principles of cortical organization, such as the ones discussed in the previous section. In contrast, area 35 of the perirhinal cortex exhibits a different laminar profile, its deep layers being relatively more developed than its superficial layers. Such differences may be linked to topographical constraints given its location in the depths of the rhinal sulcus. Note that similar laminar proportions are observed in other cortical areas in monkeys, including area 29 of the retrosplenial cortex, which is also located in the depths of a sulcus (Zilles et al. 1986), and area 13 of the orbitofrontal cortex (Semendeferi et al. 1998). The functional implications of this organization remain to be determined.

The perirhinal and parahippocampal cortices provide about two-thirds of the cortical inputs to the entorhinal cortex (Insausti, Amaral, and Cowan 1987; Suzuki and Amaral 1994b). These projections originate predominantly in layers III, which together contain 3.96 million neurons, or about 30% of the total number of neurons contained in the perirhinal and parahippocampal cortices, and terminate in the superficial layers I–III of the entorhinal cortex, which together contain 2.12 million neurons, or about 60% of the total number of neurons in this cortex (Piguet et al. 2018). These numbers suggest a strong convergence and integration of information within the entorhinal cortex, the intrinsic connections of which are organized in separate associational networks and are preferentially interconnected with different rostrocaudal portions of the hippocampus (Chrobak and Amaral 2007). Consistent with the fact that they contribute to distinct functional circuits, perirhinal inputs mainly converge in the superficial layers of the rostral entorhinal cortex, whereas parahippocampal inputs converge in the superficial layers of the caudal entorhinal cortex (Suzuki and Amaral 1994b). The feedback projections from the entorhinal cortex to the perirhinal and parahippocampal cortices follow the same rostrocaudal organization as the feedforward projections (Suzuki and Amaral 1994b). They originate in layers V and VI of the entorhinal cortex, which contain 1.41 million neurons, or about 40% of the neurons in the entorhinal cortex, and terminate mostly in superficial but also deep layers of the perirhinal and parahippocampal cortices.

Interestingly, when considering perirhinal and parahippocampal areas (36r, 36c, TH, and TF) as well as the distinct entorhinal subdivisions, the ratio of the number of neurons located in the superficial versus deep layers was higher in rostromedial subdivisions compared to caudolateral subdivisions (Figure 5). This trend is consistent with the degree of reciprocal connections both within and between the entorhinal, perirhinal, and parahippocampal cortices (Chrobak and Amaral 2007; Lavenex, Suzuki, and Amaral 2004; Suzuki and Amaral 1994b). The higher ratios in areas Eo and Er are consistent with the limited interconnections of area Eo with adjacent entorhinal fields (Chrobak and Amaral 2007), as well as the fact that the projections between the perirhinal cortex and the entorhinal cortex are less reciprocal: That is, there are more feedforward projections from the perirhinal cortex to the rostral portion of the entorhinal cortex than there are feedback projections from the rostral entorhinal cortex to the perirhinal cortex (Suzuki and Amaral 1994b). In contrast, the lower ratios in the caudal subdivisions of the entorhinal cortex and in areas 36r, 36c, TH, and TF of the perirhinal and parahippocampal cortices are consistent with the more reciprocal connections between the perirhinal cortex and parahippocampal cortex and between the parahippocampal cortex and the caudal portion of the entorhinal cortex (Lavenex, Suzuki, and Amaral 2004; Suzuki and Amaral 1994b). In sum, there are rostrocaudal and mediolateral gradients in the ratio of the number of neurons located in the superficial versus deep layers both in the entorhinal cortex and in the perirhinal and parahippocampal cortices, which appear associated with the degree of reciprocity of the interconnections of these areas within the medial temporal lobe memory circuits.

Feedback projections from the perirhinal and parahippocampal cortices originate in layers V and VI, which together contain about 4.45 million neurons or about 34% of the neurons in these cortices, and are primarily directed toward the superficial layers of the neocortex (Lavenex, Suzuki, and Amaral 2002; Webster, Ungerleider, and Bachevalier 1991). With respect to these projections, it is interesting to note that whereas the parahippocampal cortex has largely reciprocal connections with the neocortex, the perirhinal cortex has more asymmetric connections (Lavenex, Suzuki, and Amaral 2002), suggesting that the different types of information processed by those cortices may necessitate different types of feedback projections to the neocortex. In particular, the processing of visuospatial information may necessitate strong reciprocal cortical connections. Here again, the ratios of the number of neurons located in the superficial versus deep layers in the perirhinal and parahippocampal cortices parallel the degree of reciprocity of the interconnections of these areas with the neocortex.

4.3 | Expansion of the Primate Perirhinal and Parahippocampal Cortices

The comparison of our results in monkeys with available data on the perirhinal and parahippocampal/postrhinal cortices in rats (Burwell and Amaral 1998; Rapp et al. 2002) and humans (Chareyron et al. 2024; Insausti et al. 1998; Noulhiane et al. 2006; Pruessner et al. 2002; Sim et al. 2006) revealed important species differences (Table 3). Notably, the monkey perirhinal cortex is 17 times larger and has 19 times more neurons than the rat perirhinal cortex. The monkey parahippocampal cortex is 30 times larger and has 64 times more neurons than the rat postrhinal cortex. In humans, the perirhinal cortex is 21 times larger and the parahippocampal cortex 24 times larger than in monkeys. Beyond the expected species differences in absolute volumes and neuron numbers, the relative sizes of the entorhinal, perirhinal, and parahippocampal cortices differ (Figure 8) and corroborate previous observations made by Burwell, Witter, and Amaral (1995) based on unfolded two-dimensional maps. In rats, the entorhinal cortex represents over 63% of the entire volume occupied by these three cortices, while the perirhinal cortex occupies 25% and the postrhinal cortex only 12%. In contrast, in monkeys, the entorhinal cortex represents only 34% of the entire volume occupied by these three cortices, and in humans only 26%. The perirhinal cortex represents 35% of the volume occupied by these three cortices in monkeys and 37% in humans. Finally, the parahippocampal cortex represents 31% of the volume occupied by these three cortices in monkeys and 37% in humans.

These differences in proportions are interesting when put in relation to the types of information processed by these cortices in rodents and primates. Indeed, although the overall connectivity patterns of the entorhinal, perirhinal, and parahippocampal–postrhinal cortices are preserved across species, some differences exist regarding the predominance of unimodal sensory inputs. In rats, the entorhinal, perirhinal, and postrhinal cortices receive more substantial inputs from olfactory areas (Burwell and Amaral 1998), particularly the entorhinal cortex, which receives direct inputs from the olfactory bulb (Kosel, Van Hoesen, and West 1981; Price 1973). Moreover, whereas these inputs reach a large portion of the rat entorhinal cortex, they only reach 15% of the monkey entorhinal cortex and 4.6% of the human entorhinal cortex (Insausti et al. 2002). In rats, the perirhinal cortex receives input from all sensory modalities (Burwell and Amaral 1998), whereas in monkeys it receives its largest input from visual areas (Suzuki and Amaral 1994a). Similar to monkeys, the rat postrhinal cortex receives its heaviest inputs from visual associative areas (Burwell and Amaral 1998; Suzuki and Amaral 1994a). Finally, the increase in relative size of the perirhinal and parahippocampal cortices parallels the cortical expansion observed in primates. Indeed, the cerebral cortex accounts for about 80% of the total brain mass in macaques and 82% in humans (Azevedo et al. 2009; Herculano-Houzel et al. 2007). In comparison, the rat cerebral cortex only accounts for about 43% of the total brain mass (Herculano-Houzel, Mota, and Lent 2006). More specifically, given the well-developed visual system in primates (Kaas 2012; Rosa and Krubitzer 1999), the perirhinal and parahippocampal cortices parallel the development of visual associative areas to which they are strongly interconnected.

5 | Conclusion

The aim of the current study was to provide reliable estimates of the basic neuroanatomical characteristics of the monkey perirhinal and parahippocampal cortices, including the volume, neuron number, and neuronal soma size in their different layers and subdivisions. The laminar organization of these areas supports the view that high-order association cortices are characterized by

TABLE 3 | Neuron number and volume of entorhinal, perirhinal, and parahippocampal/postrhinal cortices in rats, monkeys, and humans.

	Entorhinal cortex[a]		Perirhinal cortex		Parahippocampal/ Postrhinal cortex		Ento + Peri + Para/Post cortices
	Mean	SD	Mean	SD	Mean	SD	
Neuron number							
Rat (a)	640,703	49,337	303,540	47,671	112,900	34,761	1,057,143
Monkey (b, c)	3,532,411	252,997	5,865,147	1,109,303	7,185,991	732,814	16,583,549
Ratio M/R	*5.5*		*19.3*		*63.6*		*15.7*
Volume (mm^3)							
Rat (d)	16.82	2.66	6.56	1.20	3.26	0.95	26.64
Monkey (b, c)	106.92	10.77	111.93	22.23	98.22	14.97	317.07
Human[b] (e)	1,663	335	2,542	669			
Human[b] (f)	1,613	383	2,460	672	2,572	400	
Human[b] (g)	1,325	172	2,358	426	2,469	320	
Human[b] (h)	1,863	416	1,862	436	2,626	437	
Human[b] (i)	1,499	66	2,271	90	1,623	97	
Average	1,593		2,299		2,323		6,214
Ratio M/R	*6.4*		*17.1*		*30.1*		*11.9*
Ratio H/R	*94.7*		*350.4*		*712.4*		*233.2*
Ratio H/M	*14.9*		*20.5*		*23.6*		*19.6*

Note: (a) Rapp et al. (2002); (b) Piguet et al. (2018); (c) Villard et al. (2023); (d) Burwell et al. (1995); (e) Insausti et al. (1998); (f) Pruessner et al. (2002); (g) Nouhliane et al. (2006); (h) Sim et al. (2006); (i) Chareyron et al. (2024).

[a]More detailed information for the entorhinal cortex is available in Piguet et al. (2018).

[b]Volumes correspond to the average between the two hemispheres.

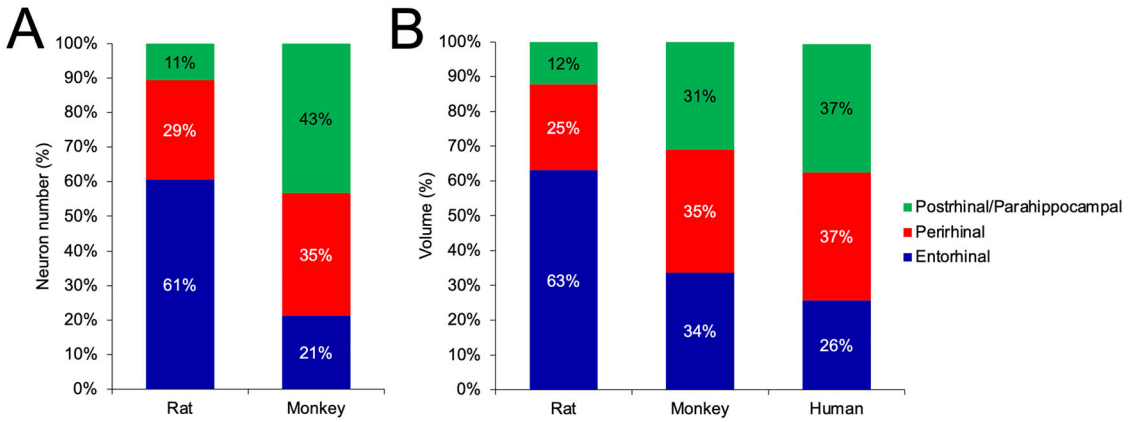

FIGURE 8 | Species comparison of the number of neurons and volume of the entorhinal, perirhinal, and parahippocampal cortices, expressed in percentage of the total number of neurons or volume of the three cortices (see Table 3 for references).

relatively large or thick superficial layers, overall larger neurons, and lower neuronal density. These morphological characteristics are also consistent with the hierarchical organization of these cortices within medial temporal lobe circuits and corroborate previous suggestions that although the two cortices are generally considered to be at the same hierarchical level, in between various cortical areas and the entorhinal cortex, the perirhinal cortex may be at a slightly higher level than the parahippocampal cortex. Finally, when compared to findings in rats and humans, our data in monkeys revealed important species differences and confirmed earlier suggestions that the relative size and number of neurons of the entorhinal, perirhinal, and parahippocampal cortices reflect the relative development of interconnected brain structures, and that the perirhinal and parahippocampal cortices parallel cortical expansion in primates. Altogether, these normative data provide an essential reference to extrapolate findings from experimental studies in animals and create realistic models of the medial temporal lobe memory system.

Acknowledgments

This work was supported by the Swiss National Science Foundation (Grants P00A-106701, PP00P3-124536, and 310030_143956), US National Institutes of Health (Grants MH041479 and NS16980), and the California National Primate Research Center (Grant OD011107). We thank the CNPRC staff, Jeff Bennett, Grégoire Favre, Jane Favre, Adeline Jabès, Olivia Piguet, Danièle Uldry, and K.C. Wells for technical assistance at various stages of the project. We thank Peter Rapp and Rebecca Burwell for providing data in rats.

Conflicts of Interest

The authors declare no conflicts of interest.

Data Availability Statement

The data that support the findings of this study are available from the corresponding author upon reasonable request.

Peer Review

The peer review history for this article is available at https://publons.com/publon/10.1002/cne.25684

References

Agster, K. L., and R. D. Burwell. 2009. "Cortical Efferents of the Perirhinal, Postrhinal, and Entorhinal Cortices of the Rat." *Hippocampus* 19, no. 12: 1159–1186. https://doi.org/10.1002/hipo.20578.

Amaral, D. G., and P. Lavenex. 2007. Hippocampal Neuroanatomy. In *The Hippocampus Book*, edited by D. G. Amaral, P. Andersen, T. Bliss, R. G. M. Morris, and J. O'Keefe, 37–114. New York: Oxford University Press.

Augustinack, J. C., K. E. Huber, A. A. Stevens, et al. 2013. "Predicting the Location of human Perirhinal Cortex, Brodmann's Area 35, From MRI." *Neuroimage* 64: 32–42. https://doi.org/10.1016/j.neuroimage.2012.08.071.

Azevedo, F. A., L. R. Carvalho, L. T. Grinberg, et al. 2009. "Equal Numbers of Neuronal and Nonneuronal Cells Make the Human Brain an Isometrically Scaled-Up Primate Brain." *Journal of Comparative Neurology* 513, no. 5: 532–541. https://doi.org/10.1002/cne.21974.

Barbas, H. 1986. "Pattern in the Laminar Origin of Corticocortical Connections." *Journal of Comparative Neurology* 252, no. 3: 415–422. https://doi.org/10.1002/cne.902520310.

Barbas, H., and N. Rempel-Clower. 1997. "Cortical Structure Predicts the Pattern of Corticocortical Connections." *Cerebral Cortex* 7, no. 7: 635–646. https://doi.org/10.1093/cercor/7.7.635.

Barense, M. D., and A. C. H. Lee. 2021. "Perception and Memory in the Medial Temporal Lobe: Deep Learning Offers a New Lens on an Old Debate." *Neuron* 109, no. 17: 2643–2645. https://doi.org/10.1016/j.neuron.2021.08.018.

Basler, L., S. Gerdes, D. P. Wolfer, and L. Slomianka. 2017. "Sampling the Mouse Hippocampal Dentate Gyrus." *Frontiers in Neuroanatomy* 11: 123. https://doi.org/10.3389/fnana.2017.00123.

Bautista, J., M. A. Garcia-Cabezas, M. Medalla, D. L. Rosene, B. Zikopoulos, and H. Barbas. 2023. "Pattern of Ventral Temporal Lobe Interconnections in rhesus Macaques." *Journal of Comparative Neurology* 531, no. 18: 1963–1986. https://doi.org/10.1002/cne.25550.

Blaizot, X., F. Mansilla, A. M. Insausti, et al. 2010. "The Human Parahippocampal Region: I. Temporal Pole Cytoarchitectonic and MRI Correlation." *Cerebral Cortex* 20, no. 9: 2198–2212. https://doi.org/10.1093/cercor/bhp289.

Blatt, G. J., D. N. Pandya, and D. L. Rosene. 2003. "Parcellation of Cortical Afferents to Three Distinct Sectors in the Parahippocampal Gyrus of the Rhesus Monkey: An Anatomical and Neurophysiological Study." *Journal of Comparative Neurology* 466, no. 2: 161–179. https://doi.org/10.1002/cne.10866.

Braak, H., and E. Braak. 1985. "On Areas of Transition Between Entorhinal Allocortex and Temporal Isocortex in the Human Brain. Normal Morphology and Lamina-Specific Pathology in Alzheimer's Disease." *Acta Neuropathologica* 68, no. 4: 325–332. https://doi.org/10.1007/BF00690836.

Burwell, R. D. 2001. "Borders and Cytoarchitecture of the Perirhinal and Postrhinal Cortices in the Rat." *Journal of Comparative Neurology* 437, no. 1: 17–41. https://doi.org/10.1002/cne.1267.

Burwell, R. D., and D. G. Amaral. 1998. "Cortical Afferents of the Perirhinal, Postrhinal, and Entorhinal Cortices of the Rat." *Journal of Comparative Neurology* 398, no. 2: 179–205. https://doi.org/10.1002/(sici)1096-9861(19980824)398:2⟨179::aid-cne3⟩3.0.co;2-y.

Burwell, R. D., M. P. Witter, and D. G. Amaral. 1995. "Perirhinal and Postrhinal Cortices of the Rat: A Review of the Neuroanatomical Literature and Comparison With Findings From the Monkey Brain." *Hippocampus* 5, no. 5: 390–408. https://doi.org/10.1002/hipo.450050503.

Chareyron, L. J., D. G. Amaral, and P. Lavenex. 2016. "Selective Lesion of the Hippocampus Increases the Differentiation of Immature Neurons in the Monkey Amygdala." *Proceedings of the National Academy of Sciences of the United States of America* 113, no. 50: 14420–14425. https://doi.org/10.1073/pnas.1604288113.

Chareyron, L. J., P. Banta Lavenex, D. G. Amaral, and P. Lavenex. 2011. "Stereological Analysis of the Rat and Monkey Amygdala." *Journal of Comparative Neurology* 519, no. 16: 3218–3239. https://doi.org/10.1002/cne.22677.

Chareyron, L. J., P. Banta Lavenex, D. G. Amaral, and P. Lavenex. 2012. "Postnatal Development of the Amygdala: A Stereological Study in Macaque Monkeys." *Journal of Comparative Neurology* 520, no. 9: 1965–1984. https://doi.org/10.1002/cne.23023.

Chareyron, L. J., P. Banta Lavenex, D. G. Amaral, and P. Lavenex. 2021. "Life and Death of Immature Neurons in the Juvenile and Adult Primate Amygdala." *International Journal of Molecular Sciences* 22, no. 13: 6691. https://doi.org/10.3390/ijms22136691.

Chareyron, L. J., W. K. K. Chong, T. Banks, N. Burgess, R. C. Saunders, and F. Vargha-Khadem. 2024. "Anatomo-Functional Changes in Neural Substrates of Cognitive Memory in Developmental Amnesia: Insights From Automated and Manual Magnetic Resonance Imaging Examinations." *Hippocampus* 34: 645–658. https://doi.org/10.1002/hipo.23638.

Chrobak, J. J., and D. G. Amaral. 2007. "Entorhinal Cortex of the Monkey: VII. Intrinsic Connections." *Journal of Comparative Neurology* 500, no. 4: 612–633. https://doi.org/10.1002/cne.21200.

de Sousa, A. A., C. C. Sherwood, A. Schleicher, et al. 2010. "Comparative Cytoarchitectural Analyses of Striate and Extrastriate Areas in Hominoids." *Cerebral Cortex* 20, no. 4: 966–981. https://doi.org/10.1093/cercor/bhp158.

Ding, S. L., and G. W. Van Hoesen. 2010. "Borders, Extent, and Topography of human Perirhinal Cortex as Revealed Using Multiple Modern Neuroanatomical and Pathological Markers." *Human Brain Mapping* 31, no. 9: 1359–1379. https://doi.org/10.1002/hbm.20940.

Ding, S. L., G. W. Van Hoesen, M. D. Cassell, and A. Poremba. 2009. "Parcellation of Human Temporal Polar Cortex: A Combined Analysis of Multiple Cytoarchitectonic, Chemoarchitectonic, and Pathological Markers." *Journal of Comparative Neurology* 514, no. 6: 595–623. https://doi.org/10.1002/cne.22053.

Elston, G. N., R. Benavides-Piccione, and J. Defelipe. 2005. "A Study of Pyramidal Cell Structure in the Cingulate Cortex of the Macaque Monkey With Comparative Notes on Inferotemporal and Primary Visual Cortex." *Cerebral Cortex* 15, no. 1: 64–73. https://doi.org/10.1093/cercor/bhh109.

Elston, G. N., and M. G. Rosa. 1997. "The Occipitoparietal Pathway of the Macaque Monkey: Comparison of Pyramidal Cell Morphology in Layer III of Functionally Related Cortical Visual Areas." *Cerebral Cortex* 7, no. 5: 432–452. https://doi.org/10.1093/cercor/7.5.432.

Elston, G. N., and M. G. Rosa. 1998. "Morphological Variation of Layer III Pyramidal Neurones in the Occipitotemporal Pathway of the Macaque

Monkey Visual Cortex." *Cerebral Cortex* 8, no. 3: 278–294. https://doi.org/10.1093/cercor/8.3.278.

Felleman, D. J., A. Burkhalter, and D. C. Van Essen. 1997. "Cortical Connections of Areas V3 and VP of Macaque Monkey Extrastriate Visual Cortex." *Journal of Comparative Neurology* 379, no. 1: 21–47. https://doi.org/10.1002/(sici)1096-9861(19970303)379:1⟨21::aid-cne3⟩3.0.co;2-k.

Felleman, D. J., and D. C. Van Essen. 1991. "Distributed Hierarchical Processing in the Primate Cerebral Cortex." *Cerebral Cortex* 1, no. 1: 1–47. https://doi.org/10.1093/cercor/1.1.1-a.

Furtak, S. C., S. Wei, K. L. Agster, and R. D. Burwell. 2007. "Functional Neuroanatomy of the Parahippocampal Region in the Rat: The Perirhinal and Postrhinal Cortices." *Hippocampus* 17, no. 9: 709–722. https://doi.org/10.1002/hipo.20314.

Garcia-Cabezas, M. A., H. Barbas, and B. Zikopoulos. 2018. "Parallel Development of Chromatin Patterns, Neuron Morphology, and Connections: Potential for Disruption in Autism." *Frontiers in Neuroanatomy* 12: 70. https://doi.org/10.3389/fnana.2018.00070.

Garcia-Cabezas, M. A., J. L. Hacker, and B. Zikopoulos. 2023. "Homology of Neocortical Areas in Rats and Primates Based on Cortical Type Analysis: An Update of the Hypothesis on the Dual Origin of the Neocortex." *Brain Structure and Function* 228, no. 5: 1069–1093. https://doi.org/10.1007/s00429-022-02548-0.

García-Cabezas, M. Á., Y. J. John, H. Barbas, and B. Zikopoulos. 2016. "Distinction of Neurons, Glia and Endothelial Cells in the Cerebral Cortex: An Algorithm Based on Cytological Features." *Frontiers in Neuroanatomy* 10: 107. https://doi.org/10.3389/fnana.2016.00107.

Gundersen, H. J. 1988. "The Nucleator." *Journal of Microscopy* 151, no. 1: 3–21. https://doi.org/10.1111/j.1365-2818.1988.tb04609.x.

Gundersen, H. J., and E. B. Jensen. 1987. "The Efficiency of Systematic Sampling in Stereology and Its Prediction." *Journal of Microscopy* 147, no. Pt 3: 229–263. https://doi.org/10.1111/j.1365-2818.1987.tb02837.x.

Gundersen, H. J., E. B. Jensen, K. Kieu, and J. Nielsen. 1999. "The Efficiency of Systematic Sampling in Stereology–Reconsidered." *Journal of Microscopy* 193, no. Pt 3: 199–211. https://doi.org/10.1046/j.1365-2818.1999.00457.x.

Herculano-Houzel, S., C. E. Collins, P. Wong, and J. H. Kaas. 2007. "Cellular Scaling Rules for Primate Brains." *Proceedings of the National Academy of Sciences of the United States of America* 104, no. 9: 3562–3567. https://doi.org/10.1073/pnas.0611396104.

Herculano-Houzel, S., B. Mota, and R. Lent. 2006. "Cellular Scaling Rules for Rodent Brains." *Proceedings of the National Academy of Sciences of the United States of America* 103, no. 32: 12138–12143. https://doi.org/10.1073/pnas.0604911103.

Hilgetag, C. C., and A. Goulas. 2020. "Hierarchy' in the Organization of Brain Networks." *Philosophical Transactions of the Royal Society of London. Series B: Biological Sciences* 375, no. 1796: 20190319. https://doi.org/10.1098/rstb.2019.0319.

Hilgetag, C. C., M. Medalla, S. F. Beul, and H. Barbas. 2016. "The Primate Connectome in Context: Principles of Connections of the Cortical Visual System." *Neuroimage* 134: 685–702. https://doi.org/10.1016/j.neuroimage.2016.04.017.

Insausti, R., D. G. Amaral, and W. M. Cowan. 1987. "The Entorhinal Cortex of the Monkey: II. Cortical Afferents." *Journal of Comparative Neurology* 264, no. 3: 356–395. https://doi.org/10.1002/cne.902640306.

Insausti, R., K. Juottonen, H. Soininen, et al. 1998. "MR Volumetric Analysis of the Human Entorhinal, Perirhinal, and Temporopolar Cortices." *AJNR American Journal of Neuroradiology* 19, no. 4: 659–671. https://www.ajnr.org/content/19/4/659.

Insausti, R., P. Marcos, M. M. Arroyo-Jimenez, X. Blaizot, and A. Martinez-Marcos. 2002. "Comparative Aspects of the Olfactory Portion of the Entorhinal Cortex and Its Projection to the Hippocampus in Rodents, Nonhuman Primates, and the Human Brain." *Brain Research Bulletin* 57, no. 3–4: 557–560. https://doi.org/10.1016/s0361-9230(01)00684-0.

Jabès, A., P. Banta Lavenex, D. G. Amaral, and P. Lavenex. 2010. "Quantitative Analysis of Postnatal Neurogenesis and Neuron Number in the Macaque Monkey Dentate Gyrus." *European Journal of Neuroscience* 31, no. 2: 273–285. https://doi.org/10.1111/j.1460-9568.2009.07061.x.

Jabès, A., P. Banta Lavenex, D. G. Amaral, and P. Lavenex. 2011. "Postnatal Development of the Hippocampal Formation: A Stereological Study in Macaque Monkeys." *Journal of Comparative Neurology* 519, no. 6: 1051–1070. https://doi.org/10.1002/cne.22549.

Kaas, J. H. 2012. "The Evolution of Neocortex in Primates." *Progress in Brain Research* 195: 91–102. https://doi.org/10.1016/B978-0-444-53860-4.00005-2.

Knierim, J. J., J. P. Neunuebel, and S. S. Deshmukh. 2014. "Functional Correlates of the Lateral and Medial Entorhinal Cortex: Objects, Path Integration and Local-Global Reference Frames." *Philosophical Transactions of the Royal Society of London. Series B: Biological Sciences* 369, no. 1635: 20130369. https://doi.org/10.1098/rstb.2013.0369.

Kosel, K. C., G. W. Van Hoesen, and J. R. West. 1981. "Olfactory Bulb Projections to the Parahippocampal Area of the Rat." *Journal of Comparative Neurology* 198, no. 3: 467–482. https://doi.org/10.1002/cne.901980307.

Lavenex, P., and D. G. Amaral. 2000. "Hippocampal-Neocortical Interaction: A Hierarchy of Associativity." *Hippocampus* 10, no. 4: 420–430. https://doi.org/10.1002/1098-1063(2000)10:4⟨420::AID-HIPO8⟩3.0.CO;2-5.

Lavenex, P., P. Banta Lavenex, J. L. Bennett, and D. G. Amaral. 2009. "Postmortem Changes in the Neuroanatomical Characteristics of the Primate Brain: The Hippocampal Formation." *Journal of Comparative Neurology* 512, no. 1: 27–51. https://doi.org/10.1002/cne.21906.

Lavenex, P., W. A. Suzuki, and D. G. Amaral. 2002. "Perirhinal and Parahippocampal Cortices of the Macaque Monkey: Projections to the Neocortex." *Journal of Comparative Neurology* 447, no. 4: 394–420. https://doi.org/10.1002/cne.10243.

Lavenex, P., W. A. Suzuki, and D. G. Amaral. 2004. "Perirhinal and Parahippocampal Cortices of the Macaque Monkey: Intrinsic Projections and Interconnections." *Journal of Comparative Neurology* 472, no. 3: 371–394. https://doi.org/10.1002/cne.20079.

Maass, A., D. Berron, L. A. Libby, C. Ranganath, and E. Duzel. 2015. "Functional Subregions of the Human Entorhinal Cortex." *Elife* 4: e06426. https://doi.org/10.7554/eLife.06426.

Miyashita, Y. 2019. "Perirhinal Circuits for Memory Processing." *Nature Reviews Neuroscience* 20, no. 10: 577–592. https://doi.org/10.1038/s41583-019-0213-6.

Murray, E. A., and B. J. Richmond. 2001. "Role of Perirhinal Cortex in Object Perception, Memory, and Associations." *Current Opinion in Neurobiology* 11, no. 2: 188–193. https://doi.org/10.1016/s0959-4388(00)00195-1.

Navarro Schroder, T., K. V. Haak, N. I. Zaragoza Jimenez, C. F. Beckmann, and C. F. Doeller. 2015. "Functional Topography of the Human Entorhinal Cortex." *Elife* 4: e06738. https://doi.org/10.7554/eLife.06738.

Noulhiane, M., S. Samson, S. Clemenceau, D. Dormont, M. Baulac, and D. Hasboun. 2006. "A Volumetric MRI Study of the Hippocampus and the Parahippocampal Region After Unilateral Medial Temporal Lobe Resection." *Journal of Neuroscience Methods* 156, no. 1–2: 293–304. https://doi.org/10.1016/j.jneumeth.2006.02.021.

Peruzzi, D. 2012. *Study* Review*: Dr. Daniel Peruzzi Highlights Best Publication Practices by Analyzing a New Stereological Study*. Williston, VT, USA: MBF Bioscience. https://www.mbfbioscience.com/blog/2012/09/study-review-dr-daniel-peruzzi-highlights-best-publication-practices-by-analyzing-a-new-stereological-study/.

Piguet, O., L. J. Chareyron, P. Banta Lavenex, D. G. Amaral, and P. Lavenex. 2018. "Stereological Analysis of the Rhesus Monkey Entorhinal Cortex." *Journal of Comparative Neurology* 526, no. 13: 2115–2132. https://doi.org/10.1002/cne.24496.

Piguet, O., L. J. Chareyron, P. Banta Lavenex, D. G. Amaral, and P. Lavenex. 2020. "Postnatal Development of the Entorhinal Cortex: A Stereological Study in Macaque Monkeys." *Journal of Comparative Neurology* 528: 2308–2332. https://doi.org/10.1002/cne.24897.

Price, J. L. 1973. "An Autoradiographic Study of Complementary Laminar Patterns of Termination of Afferent Fibers to the Olfactory Cortex." *Journal of Comparative Neurology* 150, no. 1: 87–108. https://doi.org/10.1002/cne.901500105.

Pruessner, J. C., S. Kohler, J. Crane, et al. 2002. "Volumetry of Temporopolar, Perirhinal, Entorhinal and Parahippocampal Cortex From High-Resolution MR Images: Considering the Variability of the Collateral Sulcus." *Cerebral Cortex* 12, no. 12: 1342–1353. https://doi.org/10.1093/cercor/12.12.1342.

Rapp, P. R., P. S. Deroche, Y. Mao, and R. D. Burwell. 2002. "Neuron Number in the Parahippocampal Region Is Preserved in Aged Rats With Spatial Learning Deficits." *Cerebral Cortex* 12, no. 11: 1171–1179. https://doi.org/10.1093/cercor/12.11.1171.

Reznik, D., R. Trampel, N. Weiskopf, M. P. Witter, and C. F. Doeller. 2023. "Dissociating Distinct Cortical Networks Associated With Subregions of the Human Medial Temporal Lobe Using Precision Neuroimaging." *Neuron* 111: 2756–2772.e7. https://doi.org/10.1016/j.neuron.2023.05.029.

Rosa, M. G., and L. A. Krubitzer. 1999. "The Evolution of Visual Cortex: Where is V2?" *Trends in Neuroscience (Tins)* 22, no. 6: 242–248. https://doi.org/10.1016/s0166-2236(99)01398-3.

Semendeferi, K., E. Armstrong, A. Schleicher, K. Zilles, and G. W. Van Hoesen. 1998. "Limbic Frontal Cortex in Hominoids: A Comparative Study of Area 13." *American Journal of Physical Anthropology* 106, no. 2: 129–155. https://doi.org/10.1002/(SICI)1096-8644(199806)106:2⟨129::AID-AJPA3⟩3.0.CO;2-L.

Semendeferi, K., E. Armstrong, A. Schleicher, K. Zilles, and G. W. Van Hoesen. 2001. "Prefrontal Cortex in Humans and Apes: A Comparative Study of Area 10." *American Journal of Physical Anthropology* 114, no. 3: 224–241. https://doi.org/10.1002/1096-8644(200103)114:3⟨224::AID-AJPA1022⟩3.0.CO;2-I.

Sherwood, C. C., R. L. Holloway, J. M. Erwin, A. Schleicher, K. Zilles, and P. R. Hof. 2004. "Cortical Orofacial Motor Representation in Old World Monkeys, Great Apes, and Humans. I. Quantitative Analysis of Cytoarchitecture." *Brain Behavior and Evolution* 63, no. 2: 61–81. https://doi.org/10.1159/000075672.

Sim, K., I. DeWitt, T. Ditman, et al. 2006. "Hippocampal and Parahippocampal Volumes in Schizophrenia: A Structural MRI Study." *Schizophrenia Bulletin* 32, no. 2: 332–340. https://doi.org/10.1093/schbul/sbj030.

Slomianka, L. 2021. "Basic Quantitative Morphological Methods Applied to the Central Nervous System." *Journal of Comparative Neurology* 529, no. 4: 694–756. https://doi.org/10.1002/cne.24976.

Squire, L. R., and S. M. Zola. 1996. "Structure and Function of Declarative and Nondeclarative Memory Systems." *Proceedings of the National Academy of Sciences of the United States of America* 93, no. 24: 13515–13522. https://doi.org/10.1073/pnas.93.24.13515.

Stefanacci, L., W. A. Suzuki, and D. G. Amaral. 1996. "Organization of Connections Between the Amygdaloid Complex and the Perirhinal and Parahippocampal Cortices in Macaque Monkeys." *Journal of Comparative Neurology* 375, no. 4: 552–582. https://doi.org/10.1002/(SICI)1096-9861(19961125)375:4⟨552::AID-CNE2⟩3.0.CO;2-0.

Suzuki, W. A., and D. G. Amaral. 1990. "Cortical Inputs to the CA1 Field of the Monkey Hippocampus Originate From the Perirhinal and Parahippocampal Cortex But Not From Area TE." *Neuroscience Letters* 115, no. 1: 43–48. https://doi.org/10.1016/0304-3940(90)90515-b.

Suzuki, W. A., and D. G. Amaral. 1994a. "Perirhinal and Parahippocampal Cortices of the Macaque Monkey: Cortical Afferents." *Journal of Comparative Neurology* 350, no. 4: 497–533. https://doi.org/10.1002/cne.903500402.

Suzuki, W. A., and D. G. Amaral. 1994b. "Topographic Organization of the Reciprocal Connections Between the Monkey Entorhinal Cortex and the Perirhinal and Parahippocampal Cortices." *Journal of Neuroscience* 14, no. 3: 1856–1877. https://doi.org/10.1523/jneurosci.14-03-01856.1994.

Suzuki, W. A., and D. G. Amaral. 2003a. "Perirhinal and Parahippocampal Cortices of the Macaque Monkey: Cytoarchitectonic and Chemoarchitectonic Organization." *Journal of Comparative Neurology* 463, no. 1: 67–91. https://doi.org/10.1002/cne.10744.

Suzuki, W. A., and D. G. Amaral. 2003b. "Where are the Perirhinal and Parahippocampal Cortices? A Historical Overview of the Nomenclature and Boundaries Applied to the Primate Medial Temporal Lobe." *Neuroscience* 120, no. 4: 893–906. https://doi.org/10.1016/s0306-4522(03)00281-1.

Suzuki, W. A., and Y. Naya. 2014. "The Perirhinal Cortex." *Annual Review of Neuroscience* 37, no. 1: 39–53. https://doi.org/10.1146/annurev-neuro-071013-014207.

Thangavel, R., G. W. Van Hoesen, and A. Zaheer. 2008. "Posterior Parahippocampal Gyrus Pathology in Alzheimer's Disease." *Neuroscience* 154, no. 2: 667–676. https://doi.org/10.1016/j.neuroscience.2008.03.077.

Van Hoesen, G. W., D. L. Rosene, and M. M. Mesulam. 1979. "Subicular Input From Temporal Cortex in the Rhesus Monkey." *Science* 205, no. 4406: 608–610. https://doi.org/10.1126/science.109926.

Villard, J., L. J. Chareyron, O. Piguet, et al. 2023. "Structural Plasticity in the Entorhinal and Perirhinal Cortices Following Hippocampal Lesions in Rhesus Monkeys." *Hippocampus* 33: 1094–1112. https://doi.org/10.1002/hipo.23567.

Von Bonin, G., and P. Bailey. 1947. *The Neocortex of Macaca mulatta*. Urbana, IL: University of Illinois Press.

Von Economo, C., and G. N. Koskinas. 1929. *The Cytoarchitectonics of the Human Cerebral Cortex*. London: Oxford University Press.

Webster, M. J., L. G. Ungerleider, and J. Bachevalier. 1991. "Connections of Inferior Temporal Areas TE and TEO With Medial Temporal-Lobe Structures in Infant and Adult Monkeys." *Journal of Neuroscience* 11, no. 4: 1095–1116. https://www.ncbi.nlm.nih.gov/pubmed/2010806.

West, M. J., L. Slomianka, and H. J. G. Gundersen. 1991. "Unbiased Stereological Estimation of the Total Number of Neurons in the Subdivisions of the Rat Hippocampus Using the Optical Fractionator." *Anatomical Record* 231, no. 4: 482–497. https://doi.org/10.1002/ar.1092310411.

Zilles, K., E. Armstrong, G. Schlaug, and A. Schleicher. 1986. "Quantitative Cytoarchitectonics of the Posterior Cingulate Cortex in Primates." *Journal of Comparative Neurology* 253, no. 4: 514–524. https://doi.org/10.1002/cne.902530408.